D2-expressing neurons of the anterior paraventricular nucleus of the thalamus modulate learned aversive and safety salience.

Magdalena Miranda[1], Elsa Karam[1], Pola Tuduri[1], Loic Vaillant[1], Majda Drahmani[1], Jeanne Ster[1], Emmanuel Perisse[1,#,*] and Stéphanie Trouche[1,#,*]

[1]Institute of Functional Genomics, University of Montpellier, CNRS, INSERM,141 rue de la Cardonille, 34094 Montpellier Cedex 5, France.

[#] Correspondence: stephanie.trouche@igf.cnrs.fr and emmanuel.perisse@igf.cnrs.fr

* These authors contributed equally to this work

Keywords: avoidance, defensive strategies, safety, aversive value, salience, D2 receptor-expressing neurons, PVT.

Abstract

Associative learning provides a mean to learn appropriate valence and salience value signals that animal can later use to make appropriate value-based choices. By generalizing from prior aversive experience and comparing motivational salience signals to a current one, animals can learn the relative aversive ("better or worse than") value or relative positive safety between experiences. Yet, how such relative value signals are acquired during learning remain poorly known. The paraventricular nucleus of the thalamus (PVT) is critical for the control of salience and valence signals, therefore it is well-placed to be involved in learning relative aversive value and learned safety. Using a newly-developed conditioned place aversive task, we first uncover specific behavioral signatures associated with learning relative aversive value and learned safety, and related value-based choices. We then show that neurons expressing dopamine D2 receptor (D2+) in the anterior PVT (aPVT) rather than posterior PVT (pPVT), are preferentially recruited by both relative aversive value learning and learned safety. By employing a chemogenetic inactivation strategy, we first demonstrate a role of aPVT D2+ neurons for learning relative aversive value by regulating motivational aversive salience. Finally, we show that the same chemogenetic intervention also increases learned safety salience. Overall, our data are the first to demonstrate that aPVT D2+ neurons modulate the salience of experience independently of valence to compute adapted learned value signals during learning and promote appropriate value-based choices.

Introduction

Valence (positive or negative) and salience (e.g. intensity of a reinforcer) of behaviorally relevant signals are critical value information acquired during associative learning that animals can later use to make appropriate choices. [1–3] Nevertheless, past experience can modify how value information is acquired during learning. [4–6] By generalizing predictions [7,8] and comparing the salience of contextual/sensory signals of a prior experience with an ongoing one, animals can also learn the relative appetitive or aversive value between two experiences (i.e. whether one is better or worse than the other). [9–14] When later confronted to a choice between the two options, pre-computed values acquired during learning facilitate decision-making processes promoting more efficient and accurate value-based choices. [4] Critically, overgeneralization, leading to alteration of relative value computation, is maladaptive and serves as a major feature of fear-related disorders including post-traumatic stress disorder (PTSD). [7]

Previous studies show that learning the relative aversive value between two aversive experiences, such that one is perceived as better than the other, involves the reward system.[9,10,15] Similarly, a neutral and safe experience can acquire a relative positive value, or learned safety, when compared to a prior aversive experience, a process that also requires the reward system. [16–18] While fear generalization [6,7] and the interaction between appetitive and aversive systems [10,19–21] are likely crucial players, how the comparison of generalized predicted values and current motivational salience contribute to the encoding of relative aversive value and learned safety remains poorly understood.

The paraventricular nucleus of the thalamus (PVT) is a hub connecting the thalamus with cortical and limbic structures [22–26] that is critically involved in stimulus salience processing [27,28] and value assignment to associative stimuli. [29–32] The PVT is therefore a strong candidate structure for disentangling motivational conflicts and comparing experiences to compute appropriate relative value signals during learning. [5,23,27,32–35] Through its involvement in granting and updating the value of aversive experiences [27,34,36–40], here we hypothesize that the PVT is crucial for a correct assignment of a relative aversive value. In particular, the D2 dopamine receptor-expressing neurons (D2+) of the PVT are sensitive to valence [32] and are implicated in signaling aversive states. [32,37] In contrast, D2-non-expressing neurons (D2-) are modulated by arousal, relaying a salience signal to the cortex. [32] According to this functional dissociation, D2+ neurons could be crucial to inform a “better than expected” relative aversive value.

On the other side, the PVT is also instrumental for the correct assignment of a safe value to an experience. [40] However, it remains unclear whether D2+ neurons along the antero-posterior axis of the PVT differentially contributes to encoding of relative aversive value and learned safety.

Here, we addressed this question by designing a novel conditioned place avoidance task that allows mice to encode either relative aversive value or learned safety. In this task, mice learn to associate one context with a foot shock punishment, followed by a second context that is either punished with a shock of lower intensity (learning a relative “better” aversive value), or unpunished (learning a relative positive safety). After learning, mice are confronted to choose between the two contexts. We show that mice adapt their defensive responses to each task, exhibiting distinct behavioral signatures during learning and choice-test. Our data reveal that during learning of the second context, when comparing it to the previous aversive experience, both tasks preferentially recruit D2+ neurons in the aPVT compared to pPVT. We found that pharmacogenetic silencing of aPVT D2+ neurons during the exposure to the second context disrupt relative aversive comparison by increasing learned aversive salience leading to a suppressed preference towards the less punished-associated context during the choice-test. Consistently, when mice learn to associate two distinct contexts paired with the same shock intensity, silencing of aPVT D2+ neurons during the exposure to the second context increases the aversive salience of the experience, tilting mouse preference towards the first context during choice test. We also found that silencing aPVT D2+ neurons increases safety salience of the ongoing experience inducing enhanced preference towards the safe context during the choice test.

Taken together, our data demonstrate that aPVT D2+ neurons modulate motivational salience to enable accurate assignment of relative aversive value and learned safety during learning, thereby promoting appropriate value-based choices. These results also provide compelling evidence that PVT neuronal ensembles expressing D2 receptors, embedded in limbic circuits, are key in the evaluation process for assigning correct value signals to sensory experience during associative learning.

Results

Mice use different behavioral strategies for learned safety and relative aversive value-based learning and choice.

To study the neural circuits and mechanisms underlying learned safety and relative aversive motivational salience, we designed a novel 1-day version of the conditioned place avoidance (CPA) task (**Figures 1A** and **S1A**). In this task, mice are first subjected to a pretest session ("Pretest"), allowing them to explore two never-encountered contexts A and B (connected via a bridge) followed by two conditioning sessions ("S1" and "S2") in each context, and a test session ("Choice-test") between contexts A and B. Three groups were tested. For the control group, no shock was delivered in any context during S1 and S2. For the safe group (to study learned safety), mice received 4 electric shocks of 0.6 mA in Context A during S1 ("A+0.6"), but no shock in Context B during S2 ("B+0"). For the aversive group (to study learning relative aversive value), mice were subjected to 4 electric shocks of 0.6 mA in Context A during S1 ("A+0.6") as for the safe group, but received 4 electric shocks of 0.3 mA in Context B during S2 ("B+0.3"). As expected, no freezing was observed during Pretest in any group (**Figure S1B**). Both safe and aversive groups exhibited increased freezing levels in S1 and S2 conditioning sessions compared to the control group (**Figure S1C**). However, only mice in the aversive group showed increased freezing from S1 to S2 (**Figure 1B**), along with heightened anxiety as measured with a decreased time spent in the center during S2 (**Figure S1D**). Looking at the dynamic of freezing during S1 and S2 (**Figure S1E**), we found that freezing before the putative first shock of S2, but not S1, significantly (and similarly) increased for both safe and aversive groups compared to control group (**Figure 1C**). Increased freezing at the beginning of S2 suggests a generalized expectation based on their previous aversive experience in Context A. Importantly, while mice in both aversive and safe groups increased freezing after the 4th (and last) shock in S1 (**Figures 1D** and **S1E**), only mice in the aversive group increased freezing at the end of S2 (i.e. after receiving 4 shocks) (**Figures 1D** and **S1E**). Strikingly, we also observed tail-rattling behavior only in the aversive group immediately after each shock event in S2 (**Figure 1E; video 1**), but not S1 (**Figure S1F**). Therefore, the aversive group displayed an intense defensive response to a threat [41] after the delivery of additional shocks in S2. Overall, our results show that after the context-shock association, the number of aversive events modify mice general state and defensive response.

125 All mice were tested during a choice-test session one hour after conditioning. Importantly, mice were
126 first placed in their most preferred context (defined during Pretest), i.e. the context A_0 for the control
127 group and the most punished context $A_{0.6}$ for both safe and aversive groups. We first looked at their
128 latency to cross from context A to context B (i.e. 1st latency, **Figure S2A**). While the first latency was
129 similar between all 3 groups during the choice-test (**Figure S2A**), only mice from the aversive group
130 spent more time in the bridge before the 1st cross (**Figures 2A** and **2B**). In addition, most of mice in the
131 aversive group (10 out of 12) exhibited a "turn-back" behavior (**Figure 2C; video 2**) and a tendency for
132 more tail rattling (**Figure S2B**). Such behavioral signature is reminiscent of the "vicarious trial and error"
133 behavior with animals moving back and forth in direction of different choices at decision zones. [42,43]
134 After crossing the bridge for the first time (i.e. 1st cross), mice were allowed to explore the two contexts
135 for 15 min (as in [44,45]) (**Figure S2C**). We calculated a □CPA score comparing the time spent in each
136 context during Pretest (15 min, **Figure S2D**) vs Choice-test (15 min after 1st cross, **Figure 2D**). As
137 expected, control mice showed no preference between the two contexts during choice-test (**Figure 2D**).
138 Only mice of the safe and aversive groups reverted their initial preference and spent more time in the
139 less aversive context (**Figure 2D**), along with a reduced exploratory behavior (**Figure S2E**). This
140 preference was similar for both safe and aversive groups during the first 5 min of the test, but was
141 maintained for the aversive group throughout the choice-test (**Figure S2F**). For the aversive group, this
142 preference was accompanied with increased freezing in the bridge and context $B_{0.3}$ (**Figure 2E**), along
143 with higher stress marked by more pee and poo (**Figure S2G**). In line with these results, we found that
144 the aversive group stayed longer in the bridge after the 1st cross (**Figure 2F**) and therefore took longer
145 to go back to context $A_{0.6}$ (i.e. 2nd latency, **Figure 2G**). Mice in the aversive group therefore utilized
146 prior learning information to avoid the most punished context $A_{0.6}$ and potentially approach context $B_{0.3}$
147 [15] while being anxious and have difficulties to make a choice between the two contexts. Overall, we
148 reveal that mice adopt specific behavioral signatures induced by prior learned experience to enable
149 adapted value-based choices.
150

151 **Both learned safety and relative aversive learning recruit D2-expressing neurons in the aPVT**

152 We hypothesize that mice compare the relative saliency of the two experiences in conditioning S1 vs
153 S2 and assign a relative "better than" aversive value to Context B paired 0.3mA shocks for the aversive
154 group or a relative safety to context B unpaired for the safe group. However, how mice compare the

155 motivational salience of each experience to encode a relative (aversive or safe) value between
156 experiences and influence ensuing value-based choices is unclear. The PVT is central for modulating
157 anxiety-related conflicting appetitive-aversive information. [35,46] We therefore propose that the PVT can
158 be pivotal in the encoding of relative (aversive or safe) value. Notably, the functional antero-posterior
159 axis and expression D2 dopaminergic receptor (D2+ neurons) subdivision of the PVT in salience and
160 valence coding [32,47,48] could extricate the different motivational salience of prior and actual information
161 learned during the conditioning session S2. We first tested this hypothesis by asking whether PVT
162 neurons, in particular D2+ neurons, are differentially recruited during learning using D2-Cre:Ai14 mice
163 (see Methods). First, our *ex vivo* whole-cell recording experiments confirmed that td-Tomato (i.e. Ai14)
164 cells are responding to quinpirole (D2R-like agonist, 1μM; Action potential (AP) frequency baseline =
165 0.10 +/- 0.20 Hz, AP frequency quinpirole = 0.37 +/- 0.21 Hz, n= 5 cells, paired t-test p= 0.0047 **)
166 validating the use of this mouse line. We then performed a c-Fos immunostaining in the PVT of D2-
167 tagged animals of 3 groups: home-cage (HC), safe and aversive (**Figures 3A** and **3B**). To reflect c-Fos
168 activity at the time of the comparison between the two conditioning sessions, mice were perfused 90
169 min after the conditioning session S2. Behaviorally, we verified that both safe and aversive groups
170 showed distinct freezing patterns at the end of S2 (**Figures S3A** and **S3B**), as we previously described
171 (**Figures 1C** and **1D**). Looking at PVT c-Fos positive neurons, we found that both safe and aversive
172 groups show similar levels of activated neurons, but significantly higher compared to home-cage group
173 (**Figure 3C**). In both groups, such recruitment was more prominent in the anterior PVT (aPVT) than the
174 posterior PVT (pPVT) (**Figures 3C** and **S3C**) and incorporated a higher proportion of D2+ than D2-
175 neuronal population (**Figure 3D**). Importantly, this was not due to an overall increased D2+ cell density
176 in the aPVT, nor to a difference of D2+ cell densities between groups (**Figure S3D)**. These results
177 indicate that both learned safety and relative aversive learning recruit preferentially D2-expressing
178 neurons in the aPVT. Mice were subjected to a choice-test immediately before being perfused (**Figures**
179 **3A** and **S3E).** In line with our previous findings (**Figure 2D)**, both safe and aversive groups significantly
180 preferred the non-punished (Context B_0) or less punished compartment (Context $B_{0.3}$) during the choice-
181 test, respectively (positive □CPA score in **Figure S3E**). We also showed that, as in **Figure 2**, the relative
182 choice between the two previously (and differently) punished contexts $A_{0.6}$ and $B_{0.3}$ led mice to spend a
183 long time in the bridge likely assessing the two aversive options to make an appropriate choice (**Figure**
184 **S3F**). Considering the role of the PVT and the neuronal activation of D2+ neurons during the

185 conditioning session S2, we hypothesize that mice behavior during the choice test is tightly linked with
186 the activity of aPVT D2+ neurons during learning in S2. Accordingly, we found that in the aversive
187 group, the percentage of activated D2+ neurons of the aPVT (but not pPVT) during the conditioning
188 session S2 is negatively correlated with the time spent in the bridge (i.e. the decision zone) during the
189 choice test (**Figure 3E**). In other words, the less aPVT D2+ neurons were activated during S2, the more
190 time mice will spend in the bridge at the beginning of the choice test. Strikingly, such correlation was
191 not observed for aPVT D2-negative activated neurons (**Figure 3E**) nor for the safe group (**Figure 3F**).
192 These results strongly suggest a crucial role of aPVT D2+ neurons for learning relative aversive value
193 during conditioning to subsequently making an appropriate relative aversive value-based choice.
194
195 **aPVT D2-expressing neurons are crucial for learning relative aversive value**
196 Next, we directly tested the role of aPVT D2+ neurons for learning relative aversive value during
197 conditioning in S2. We virally injected D2-Cre mice with a Cre-dependent DREADD (hM4Di) or control
198 (mCherry) viral vector in the aPVT (**Figure 4A**). Four weeks later mice underwent the aversive CPA
199 task and were intra-peritoneally injected CNO 30 min before S2 to silence aPVT D2+ neurons when
200 mice relatively compare the previous S1 experience with the current S2 one (**Figure 4B**). To ascertain
201 the effect of viral transduction, we performed *ex vivo* whole-cell recordings in control- and hM4Di-D2-
202 expressing neurons of the aPVT, identified by their mCherry fluorescence (**Figure S4A)**. Our data
203 confirmed that bath application of 10□M CNO to aPVT brain sections expressing inhibitory DREADD
204 (hM4Di) hyperpolarizes D2+ neurons by drastically decreasing spike frequency. In contrast, bath
205 application of CNO was ineffective on aPVT D2-expressing neurons transduced with the control virus
206 mCherry (**Figure S4A)**. In line with previous reports, we also confirmed projection targets of aPVT D2+
207 neurons such as Nucleus Accumbens (NAc) and Amygdala (**Figure S4B**). [32] First and as expected,
208 both groups showed a similar preference of enclosure during Pretest before CNO injection (**Figure**
209 **S4C).** While silencing aPVT D2+ neurons prior to and during S2 did not change the amount of freezing
210 during conditioning (**Figures S4D** and **S4E**), it led to an increased tail-rattling behavior in S2
211 immediately after receiving each shock (**Figure 4C**). Moreover, while we observed a decreased
212 average distance travelled after each shock between S1 and S2 in the control mCherry, inhibiting aPVT
213 D2-expressing neurons lead to a maintenance of this distance during S2 (**Figure 4D**). Such findings
214 suggest that silencing aPVT D2+ neurons enhanced the shock perceived by the mice during S2

215 therefore increasing the aversive salience of context B+0.3. As a consequence, before their first cross
216 from context $A_{0.6}$ to context $B_{0.3}$ during the choice-test mice display a higher number of turnback (**Figure**
217 **4E**) and tail rattling (**Figure 4F**) in the bridge without changing their first latency (**Figure S4F**) nor the
218 time they spent in the bridge (**Figure S4G**). These results seem to indicate that mice perceive context
219 $B_{0.3}$ as threatening as context $A_{0.6}$. In line with this hypothesis, once mice first cross from context $A_{0.6}$ to
220 context $B_{0.3}$, the preference of the mCherry controls towards the previously less punished context $B_{0.3}$
221 was fully suppressed in hM4Di mice when aPVT D2+ neurons were inactivated during S2 (ΔCPA score
222 around 0; **Figure 4G**). We also found that hM4Di mice spent more time in the bridge after their first
223 cross from context $A_{0.6}$ to context $B_{0.3}$ (**Figure 4H**), indicating more hesitation to choose between the
224 two contexts. Moreover, mice froze less in the supposedly better option of context $B_{0.3}$ (**Figure 4I;** also
225 see **Figure 2E**) and returned to context $A_{0.6}$ faster (**Figure 4J**). Overall, our results suggest that silencing
226 aPVT D2+ neurons enhanced the aversive salience of the "B+0.3 mA" experience to reach a similar
227 aversive salience as in context A+0.6 mA. This will therefore prevent mice to learn the relative difference
228 between the two aversive experiences and to assign a relative "better than" aversive value to context
229 B+0.3 mA. In line with this hypothesis, conditioning mice to contexts A and B both paired with 0.6 mA
230 (**Figure S4H**) led to similar results with notably an increased tail rattling during S2 and a similar
231 distanced travelled after shock between S1 and S2 (**Figures S4I-L**). In addition, we observed similar
232 consequences during the choice-test with notably a ΔCPA score not different from 0 and similar freezing
233 in $A_{0.6}$, bridge and $B_{0.6}$ (**Figures S4M-R**). Considering the role of the PVT for regulating stimulus
234 salience [27,34,49–51], we propose that aPVT D2+ neurons play a critical role for maintaining the relative
235 salience between the two aversive experiences and therefore for participating to the encoding of relative
236 aversive value triggering adapted threat-related behavior.
237
238 **aPVT D2+ neurons modulate the salience of an aversive experience.**
239 To test whether silencing aPVT D2+ neurons can enhance the salience of an aversive experience we
240 conditioned mCherry and hM4Di mice to associate the two contexts A and B with the same series of
241 low 0.3 mA shock intensity and injected CNO prior to S2 to potentially enhance the aversive salience
242 of context B+0.3 mA (**Figure 5A**). Confirming our hypothesis, we found that silencing aPVT D2+
243 neurons drastically increased the number of tail rattling during S2 (**Figure 5B**) inducing a slight
244 reduction of time freezing after the 4th shock between S1 and S2 (**Figure 5C**). However, it did not modify

245 the distance travelled after shock (**Figure S5A**). Furthermore, and as previously shown in **Figure S4D**,
246 silencing aPVT D2+ neurons prior to S2 did not change mice freezing before the first shock during S2
247 (**Figure S5B**). These results indicate that mice perceive the conditioning session S2 as more aversively
248 salient therefore engaging into higher threat predicting behavior. As a consequence of context B+0.3
249 mA being perceived as more salient and therefore more aversive than context A+0.3 mA, we found that
250 hM4Di mice first placed in $A_{0.3}$ during the choice-test display more turnback in the bridge before their
251 first cross to context $B_{0.3}$ (**Figure 5D**). We also observe a strong trend toward spending more time before
252 their first cross to context $B_{0.3}$ (1st latency; **Figure 5E**) but not in the bridge (**Figure 5F**). However, hM4Di
253 mice do not display more tail rattling before their first cross to context $B_{0.3}$ (**Figure S5C**). We also found
254 that after their first cross to context $B_{0.3}$ while hM4Di mice spent the same amount of time in the bridge
255 than control (**Figure S5D**), they tend to freeze more in the bridge (**Figure 5G**) without changing the
256 latency to cross back to context $A_{0.3}$ (**Figure S5E**). Moreover, while control mice spend more time in
257 context $B_{0.3}$ (ΔCPA positive score; **Figure 5H**), hM4Di mice had not preference between the two
258 contexts (ΔCPA score not different from 0; **Figures S5F** and **5H**). This behavior is likely due to the
259 stronger aversiveness of context $B_{0.3}$ compared to that of context $A_{0.3}$. Combined with our results in
260 **Figures 4** and **S4**, we found that aPVT D2+ neurons can modulate the salience of an aversive
261 experience and therefore are essential in the comparison between the intensity of aversive experiences
262 during learning to enable correct assignment of relative aversive value crucial to promote future
263 appropriate value-based choices.
264
265 **aPVT D2+ neurons are involved in the incentive salience of learned safe experience.**
266 Our results in **Figures 3C** and **3D** strongly suggest that aPVT D2+ neurons are involved in both learned
267 relative aversive value and relative safety. PVT neurons have been shown to regulate the salience of
268 both aversive and appetitive behavior [27], a crucial information for both fear and reward learning. [17,52]
269 We therefore hypothesize that silencing aPVT D2+ neurons prior to and during S2 could also enhance
270 the salience of learned safety of context B+0 mA when it follows conditioning of context A+0.6 mA. To
271 test our hypothesis, we subjected mCherry and hM4Di mice to the safe conditioning (**Figure 1A**) and
272 injected CNO prior to conditioning S2 in context B+0 mA (**Figure 6A**). Silencing aPVT D2+ neurons
273 prior to and during S2 did not change mouse threat-related behavior during conditioning (**Figures 6B-**
274 **C** and **S6A-B**). However, mice behavior was significantly altered during the choice test between context

275 $A_{0.6}$ and B_0. As expected, threat-predicting behavior such as the number of turnback and tail-rattling
276 behavior in the bridge before going to context B_0 (i.e. before 1st cross) was unchanged (**Figures 6D-E**).
277 However, mice tend to exhibit a shorter latency to first cross to the safe enclosure B_0 (i.e. 1st latency,
278 **Figure 6F**) and a longer latency to go back to the punished context $A_{0.6}$ (**Figure 6G**), without changing
279 the time spent in the bridge after their first cross (**Figure S6C**). In addition, and in line with our
280 hypothesis, hM4Di mice exhibited a higher percentage of freezing in the safe context B_0 (**Figure 6H**)
281 as they showed a higher preference for the safe context B_0 compared to control mCherry mice (**Figures**
282 **S6D** and **6I**). This indicates that silencing aPVT D2+ neurons prior to and during S2 increased the
283 incentive salience of context B+0 mA thus inducing a higher preference towards the safe context B_0
284 during the choice test.
285
286 To make sure that silencing aPVT D2+ neurons before context B+0 mA did not assign a positive value
287 to this context during conditioning we exposed mCherry and hM4Di mice to two novel and distinct
288 contexts (C and D contexts, **Figure S6E**) without shock delivered, and injected CNO 30 min before S4
289 in context D+0. As expected, we did not find any change in any mice behavior during conditioning or
290 choice test (**Figures S6F-P**). Altogether, these findings strongly suggest that aPVT D2+ neurons
291 modulate learned safety during conditioning markedly influencing ensuing value-based choice
292 behavior.
293
294 **Discussion**
295 Our study reveals the critical role of aPVT D2-expressing neurons in modulating salience for learning
296 relative aversive value and relative positive safety to promote appropriate value-based choices. Using
297 a novel conditioned place avoidance task, we found that distinct behavioral signatures are associated
298 with learning relative aversive value and relative positive safety, and related value-based choices. We
299 then demonstrated that learning relative aversive value and relative positive safety preferentially recruit
300 aPVT D2-expressing neurons. When comparing an ongoing experience with a previous aversive one,
301 inactivating aPVT D2-expressing neurons increases the motivational salience of the ongoing
302 experience, i.e. enhancing the aversiveness or the safety of the experience. Such salience
303 enhancement modifies learning and then the selection of subsequent behavior when mice have to
304 choose between the two available options. This work provides key findings that may increase our

305 understanding of how context-dependent relative value and motivational salience are encoded in the
306 brain.
307
308 **aPVT D2+ neurons for learning relative aversive value**.
309 Extensive work focused on brain mechanisms for relative appetitive learning related to reward and gain.
310 [14,53,53,54,54–64] Surprisingly, the neural circuits underling relative aversive learning and choice remain
311 poorly understood. Here, we designed a novel 1-day conditioned place avoidance task in which mice
312 learn the association of two distinct contexts with different shock intensities, 0.6mA paired with the first
313 context and a second context with less intense 0.3mA shocks. Later, mice are confronted to a choice
314 between the two contexts. Our data showed that this relative aversive task is associated with increased
315 freezing, apparition of tail rattling and decreased time in the center during the second conditioning
316 session. Strikingly, tail rattling is a behavior typically associated with aggression in male mice before
317 fighting. [65] In our set of experiments, tail rattling may therefore be associated with a negative emotional
318 state and a reaction against a possible threat, occurring during learning (i.e. immediately after a
319 negative shock event) but also during memory retrieval (when mice need to choose between two
320 aversive contexts). Previous work has suggested a role of PVT for modulating the value and salience
321 of stimuli. [27,32] Moreover, previous studies highlighted its crucial role during motivational conflict
322 scenarios where both approach and defensive behaviors compete. [27,35,46,50] We found that
323 pharmacogenetic inactivation of aPVT D2+ neurons enhances the saliency of the ongoing aversive
324 experience demonstrated by increased tail-rattling and running immediately after each shock. Since tail
325 rattling behavior was recently shown to increase visual and auditory saliency of the mouse to predators
326 [41], our data suggest that aPVT D2+ neuronal inactivation caused a shift in the defensive behavior
327 strategy, favoring saliency-enhancing responses to threat. Our results also reveal that during the
328 relative choice between the two previously punished contexts, mice increased time spent and numerous
329 turnback when located in the bridge zone. Such behavior is reminiscent of the “Vicarious Trial and Error”
330 (VTE) phenomenon [42,66] observed at decision point when animals pause and move their head back and
331 forth to “scan” and evaluate the possible outcomes before making a choice between two or more options
332 with uncertain outcomes. [43] Importantly, VTE behavior is preferentially exhibited in hippocampal-
333 dependent tasks and during complex decision-making processes. [67–69] Given the critical role of
334 contextual information in our new relative task and the observed PVT-hippocampus anatomo-functional

335 connectivity [22], our newly designed relative aversive task can serve to expand our knowledge of the
336 neuronal circuits underlying VTE behavior.
337
338 **aPVT D2+ neurons modulate predictive signals for learning aversive value and learned safety**.
339 The PVT is widely responsive to aversive states and modulates fear-related behaviors [22,27,32,34,36,39,70–
340 72], but is also involved in appetitive associative learning [27,51] and reward-seeking behavior. [49,73,74]
341 Moreover, PVT neurons are activated by cues or contexts previously associated with positive or
342 negative emotional outcomes. [22,34–36,49,71,75–80] Here, we also designed a task in which the first context
343 is paired with 0.6 mA shocks followed by a second unpaired context, likely acquiring a learned safety.
344 [7] Our c-Fos staining revealed that the aPVT is activated by both a second context paired with a mild
345 shock (relative aversive) or the absence of shock (learned safety). As mice likely generalize expected
346 negative prediction from a previous aversive experience to learn relative aversive value or safety, our
347 results are reminiscent of previous reports showing that the omission of expected reward activates the
348 aPVT, but not the pPVT [49] The aPVT is therefore strongly involved in generating predictive value signals
349 independent of valence. To compute these predictive value signals, the PVT receives inputs from
350 regions involved in learned safety such as the infralimbic, prelimbic cortex [26,81–84] and ventral
351 hippocampus [85,86], that convey information about motivational state and arousal, respectively. To
352 modulate predictive value signals the PVT projects to the ventral tegmental area (VTA) and substantia
353 nigra pars compacta (SNc) [87] where computation of prediction error (comparison between predicted
354 and actual information) is crucial to signal correct value to sensory experience during learning.[88,89]
355 Notably VTA dopaminergic neurons expressing D2 receptors (auto-receptors) can regulate the salience
356 of threat signals. [90] As the reward system is involved is both relative aversive value [9,10] and learned
357 safety [16,18,91,92], the PVT could modulate the computation of relative value signals in the VTA. The aPVT
358 also projects to regions modulating approach-avoidance behaviors such as PFC [32,93] and ventral
359 subiculum [93], extended amygdala [93,94], nucleus accumbens (NAc) shell [25,93,95] and NAc core. Since NAc
360 integrates dopaminergic inputs from the VTA with glutamatergic inputs from the PVT [96,97], inactivation
361 of aPVT D2+ neurons could deregulate dopamine signaling in the NAc. This could potentially lead to
362 an aberrant assignment of salience to neutral stimuli [98] and therefore disrupt the ability to modulate
363 aversive and safety-related learning.

364 Furthermore, our results revealed a preferential activation of aPVT D2-expressing neurons during
365 learning relative aversive value or safety, although we and others found D2+ neurons are preferentially
366 located in the pPVT. [32,47]. Importantly, generalized threat prediction, involved here for learning relative
367 aversive value or safety, also involve the activation of D2 type receptors in both extended amygdala
368 substructures i.e.e the central amygdala and the bed nucleus of the stria terminalis BNST that have
369 been shown to contribute to anxiety-like behaviors. [99] Noteworthy, aPVT D2-expressing neurons
370 activation was tightly linked with the time spent in the bridge during choice-test, a crucial behavioral
371 hallmark of the decision-making process between different options. Indeed, the less recruited aPVT
372 D2+ neurons, but not pPVT, the more animals spent time in the bridge in the relative aversive, but not
373 safe, condition. Consistent with this observation, we found that the selective inactivation of aPVT D2-
374 expressing neurons increases the time spent in the bridge in the relatively aversive, but not the safe
375 condition, thus preventing mice to select the most appropriate behavior when facing two aversive
376 situations.
377
378 **aPVT D2+ neuronal modulation of motivational salience**
379 Emotionally salient events, regardless whether positive or negative, are encoded and remembered with
380 greater accuracy compared to emotionally neutral ones. [100–104] The PVT is involved in arousal [32,105,106]
381 and can encode salience of both conditioned and unconditioned stimuli. [27] Our results showed a role
382 for aPVT D2-expressing neurons for modulating the salience of an experience, with increasing its
383 aversiveness or its safety. It remains unclear whether the conditioned stimulus (here, the context) or
384 the outcome (shock or no shock delivered) become more salient. For the relative aversive task, such
385 manipulation increased tail rattling behavior during conditioning, but not freezing. Consistently, a recent
386 study identified that tail rattling, but not freezing behavior, positively scales with arousal level. [41]
387 Inactivation of aPVT D2-expressing neurons also increased the number of turnback and time in the
388 bridge (i.e. hesitation) during the choice-test, thus leading to the absence of preference for the less
389 punished context. Importantly, the same inactivation procedure during the safe conditioning did not
390 affect tail rattling behavior nor the time in the bridge, but it led to in an increased preference for the safe
391 context. The efficiency of the value-based choices is therefore influenced by the salience of the
392 experience and the computation and comparison of values assigned at the time of learning. [4]
393 Inactivation of aPVT D2+ neurons could have led to an incorrect value assignment during the context-

394 outcome association, thus favoring the contribution of D2-negative neurons for the attribution of
395 salience to the ongoing experience. [32,78] This could hamper (for the relative aversive task) or favor (for
396 learned safety) the ability of animals to distinguish between the options associated with each context.
397 Inactivating aPVT D2+ neurons could therefore enhance the formation of memory of any otherwise low-
398 salient stimuli.
399 Overall, our findings extend current knowledge about the role of PVT as an integrator of emotional,
400 contextual and sensory information to guide appropriate behavior. This work provides new evidence
401 about the role of aPVT D2-expressing neurons for contextual aversive learning that supports value-
402 based decisions. Here, we show that this population modulates the salience of contextual
403 cues/information, which allows mice to detect the aversiveness or safety of an experience. A better
404 understanding of neuronal circuit mechanisms responsible of the balance between value information
405 and salience is therefore critical for motivated behaviors. Indeed, an excessive stimulus evaluation
406 and/or salience processing during traumatic events (that could involve the PVT) might lead to
407 associative learning impairment and contribute to the genesis of anxiety disorders such as post-
408 traumatic stress disorder (PTSD). [107,108]
409
410 **Resource availability**
411 Further information and requests for resources and reagents should be directed to, and will be fulfilled
412 by, the lead contact, Emmanuel Perisse (emmanuel.perisse@igf.cnrs.fr) and Stéphanie Trouche
413 (stephanie.trouche@igf.cnrs.fr).
414
415 **Materials availability**
416 All original reagents presented in this study are available from the Lead Contacts upon request.
417
418 **Data and code availability**
419 All code used in this paper using Fiji will be shared by the Lead Contacts upon request.
420
421
422
423

424 **METHODS**

425 **Animals**

426 We used C57BL/6J (Charles River Laboratories, France) and three transgenic heterozygous adult male
427 mouse lines: D2-Cre mice (STOCK Tg(*Drd2*-cre) ER44Gsat/Mmucd, provided by E. Valjent), D2-
428 Cre:Ribotag mice [109] (provided by E. Valjent) and D2-Cre:Ai14 mice, that were generated by crossing
429 Drd2-Cre mice with Ai14 mice (B6.Cg-*Gt(ROSA)26Sor*$^{tm14(CAG\text{-}tdTomato)Hze}$/J, stock #007914). The latter
430 transgenic mouse line expressed the red fluorescent protein double-tomato (tdTom) under endogenous
431 regulatory elements of the D2 receptor. All transgenic mice were maintained on a C57BL/6J
432 background. Animals were housed with their littermates and were singly housed in their home cage
433 after the surgical procedure on a 12-h light/dark cycle (7 a.m. to 7 p.m.) in stable temperature (22°C)
434 and humidity (60%) conditions with free access to food and water in a dedicated housing room. Mice
435 were randomly assigned to behavioral groups. All experimental procedures were conducted in
436 agreement with the guidelines of the French Agriculture and Forestry Ministry for handling animals
437 (authorization number/license A3417241) and approved by the local and national ethic committees
438 (authorizations APAFIS #23555).

439

440 **Immunofluorescent staining and c-Fos analysis**

441 Mice (D2-Cre:Ai14 or D2-Cre:Ribotag, see Figures 3 and S3) were anaesthetized and transcardially
442 perfused with PBS followed by 4% PFA in PBS solution 90 min after the second session of conditioning
443 of the CPA task. Brains were extracted and kept in 4% PFA for at least 24 h before slicing using the
444 vibratome and coronal sections (30µm thick) were stored in PBS-azide at 4°C. For the
445 immunohistochemistry procedures, free-floating sections were rinsed extensively in PBS with 0.25%
446 Triton X-100 (PBS-T) and blocked for 1 h at room temperature in PBS-T with 10% normal donkey serum
447 (NDS). An average of 3.5 sections per animal of either aPVT or pPVT were used. Sections were then
448 incubated overnight at room temperature with primary antibodies diluted in 3% NDS blocking solution.
449 The primary antibodies used were: anti-RFP (MBL, rabbit, 1/2000, #PM005), *c-Fos* antibody (Synaptic
450 Systems, rat, 1/5000, #226017), anti-HA (rabbit, 1/500, Rockland #600-401-384). After three 15 min
451 washes using PBS, sections were incubated overnight at room temperature in PBS containing a mixture
452 of secondary antibodies. Secondary antibodies used were: donkey 488-coupled anti-rabbit (Jackson
453 Laboratory, 1/1000), donkey Cy3-coupled anti-rabbit (Jackson Laboratory #711-165-152, 1/1000),

454 donkey Cy5-coupled anti-rat (Jackson Laboratory #712-605-150, 1/1000), donkey 488-coupled anti-rat
455 (Jackson Laboratory #712-545-153, 1/500) and donkey Cy3-coupled anti-rat (Jackson Laboratory
456 #711-545-152, 1/1000). After three 15 min washes in PBS, sections were mounted on slides and stored
457 at 4°C. Images were taken using a ZEISS Apotome Microscope at 16bits and either 10X or 20X.
458 c-Fos expression was examined in D2 tagged cells using the D2-Cre:ai14 mice or D2-Cre:Ribotag (in
459 a balanced manner by group) using ImageJ based automated analysis. For each section, a region of
460 interest was assigned for both aPVT and pPVT and a threshold was selected to count both the amount
461 of c-Fos+ cells, D2+ cells and c-Fos+ D2+ colocalization. Sections from the anterior part of the PVT
462 (aPVT) were taken at AP:-0.22 to -1.22 while the posterior part of the PVT (pPVT) were taken at AP:-
463 1.34 to -2.18.
464
465 ***In vivo* pharmacogenetic inhibition**
466 For *in vivo* pharmacogenetic (Designer Receptors Exclusively Activated by Designer Drugs, DREADD)
467 inhibition in CPA experiments, Clozapine N-Oxide (2 mg/kg CNO, Enzo Life Science, #BML-NS105-
468 0025) was intraperitoneally (i.p.) injected 30 min before the second conditioning session S2.
469
470 **Stereotaxic viral injections**
471 The following adeno-associated viral vectors (AAV) were used: AAV2/1-hSyn-DIO-hM4D(Gi)-mCherry,
472 (7.1E12 vg/mL, #44362 Addgene), AAV2/1-hsyn-DIO-mCherry (1.7E13 vg/mL, #50459 Addgene). Mice
473 were anaesthetized with Isoflurane (0.5–3.5% oxygen gas mixture 2 l/min) and buprenorphine (0.1mg
474 per kg of body weight) for stereotaxic injections. Viral injections were targeted unilaterally to aPVT
475 (coordinates: AP -0.4 mm; ML -0.6 mm; DV -3.25 mm, 10° angle; 200nl per site). The viral vectors were
476 delivered at a rate of 100nl/min using a glass micropipette lowered to the target site and that remained
477 for 5min after injection before it was withdrawn. Mice were tested for behavior 4 weeks after viral
478 injections. At least 7 days before testing, animals were singled caged to prepare them for the behavioral
479 experiment.
480
481 **Behavioral procedures**
482 We developed a 1-day aversive task (Conditioned Place Avoidance, CPA, task) based on a previously
483 published conditioned place preference task. [44,45] The apparatus contained two electric grids on the

484 floor of each context and consists of two square-walled (46 cm × 46 cm × 30 cm) contexts with distinct
485 inside building block configurations. The two contexts were connected via a bridge (8-cm length, 7-cm
486 width) during both pre-test and test sessions. The access to the bridge was blocked during each
487 conditioning session. All mice were handled for at least 3 days before the first experiment and, when
488 experiments involved viral injections, habituated to the injection procedure by mock injections during
489 these days.
490 During pretest, mice freely explored the two distinct contexts (e.g. one square and one circle) for 15
491 min and their baseline (spontaneous) preference for one of the two contexts was determined. Next,
492 mice were subjected to a first 10min-conditioning session (S1), in which 4 shocks (0.6 mA or 0.3mA, at
493 198 s, 278 s, 358 s and 438 s, of 2-s duration each, as in [110]) were delivered in their most preferred
494 context (Context A, "A+0.6"). Mice returned to their homecage at the end of session S1 for 30 min.
495 During the second 10min-conditioning session S2, mice received, in their least preferred enclosure
496 (Context B), either no shock (0mA, "B+0") or 4 shocks (of 0.6 mA for "B+0.6" or 0.3mA for "B+0.3" at
497 198 s, 278 s, 358 s and 438 s, of 2-s duration each). The control group (0 vs 0) went through the two
498 sessions S1 and S2 without receiving any shock. During the choice-test session 1 hour later without
499 any shock delivered, mice were placed in their most preferred context A (as defined during pre-test)
500 and were free to visit the two enclosures for 15 min after their first cross from context A to Context B.
501 Mice that displayed more than 75% preference during pretest were excluded for the rest of the
502 procedure.
503 Mice were tracked and several behavioral parameters were measured during pre-test, conditioning and
504 choice-test. A conditioned place preference score (CPA score) was calculated for each mouse during
505 both pre-test and choice-test as in [45]. Mice that did not cross to the non-preferred context B in less than
506 25 min were excluded from further analysis (i.e. they did not perform the following 15 min choice-test).
507 CPA was calculated as $CPA = \frac{t_{non\,preferred} - t_{preferred}}{t_{non\,preferred} + t_{preferred}}$. The first latency to cross was the time the animal
508 takes to first cross from the originally preferred context A (where they were first placed) to the originally
509 non-preferred context B. The second latency to cross was the time the animal takes to cross back to
510 the preferred context A. Time in the bridge was measured during the first latency (time in the bridge
511 before first cross) and during the first 5 min after the first cross. Freezing behavior was systematically
512 measured using a custom-made software (Imetronic) and was calculated as the percentage of time for
513 which mice remained immobile for more than 2 s. The percentage of time spent freezing during the

514 entire duration of the pretest and test session were reported. For the conditioning session, the
515 percentage of freezing before the 1st shock (0-3min) and after the 4th shock (8-10min) were calculated.
516 For Fig 1B, the difference between the total percentage of freezing in S2 minus the total percentage of
517 freezing in S1 was calculated for each group (total percentage of freezing for S1 and S2 used for this
518 calculation are presented in Fig. S1). All relative measurements (ΔCPA, ΔTime in bridge, etc) were
519 calculated by subtracting Choice-test behavioral measurements with the corresponding measurement
520 during the Pre-test. For example, ΔTime in the bridge was calculated as the time spent in the bridge
521 during the first 5 min after crossing during the choice test minus the time spent in the bridge during the
522 first 5 min of the pre-test session, ie. $\Delta Time\ bridge = Time\ bridge\ Choice_{0-5min} -$
523 $Time\ bridge\ Pretest_{0-5min}$. We quantified whether the animal engaged in turn back behavior (i.e. when
524 the whole body turns at 180deg) before 1st crossing from A to B when the animal was in the bridge.
525 Tail rattling was measured as a rapid vibration of the tail either after each shock delivered during
526 conditioning sessions S1 and S2 or before the first cross during the choice test. For experiments shown
527 in Fig. S6, animals from the 0-0 control group were animals that went through the 0.3-0.3 condition one
528 week before. A different set of contexts (C and D) were used in which the floor was plain and without
529 grids. For measuring the distance travelled post shock delivery as done in [111], we averaged for each
530 conditioning session the distance travelled for 8 seconds from the time of each shock epoch (ie. 198-
531 206 s, 278-286 s, 358-366 s, 438-446 s).
532
533 **Brain slice electrophysiology**
534 Patch-clamp recordings, in whole-cell configuration, were performed on PVT D2-labeled cells in current
535 clamp mode. Briefly, D2-Cre:Ai14 mice were anesthetized and perfused intracardially with ice-cold
536 dissection buffer (25 mM NaHCO3, 1.25 mM, NaH2PO4, 2.5 mM KCl, 0.5 mM CaCL2, 7 mM MgCl2,
537 25 mM D-glucose, 110 mM choline chloride, 11.6 mM ascorbic acid, 3.1 mM Pyruvic acid maintained
538 in 5% CO2/ 95% O2). Coronal brain slices (350µm) were cut in dissection buffer using a vibratome
539 (Campden Instruments). Sections were incubated in artificial cerebrospinal fluid (ACSF) containing the
540 following (in mM) 125 NaCl, 2.7 KCl, 11.6 NaHCO3, 0.4 NaH2PO4, 1 MgCl2, 2 CaCl2, 5.6 D-glucose
541 (pH 7.4, osmolarity 305 mOsm) at 32°C for 5 min and then kept in room temperature for at least 1h
542 before recording. For the experiment, slices were superfused continuously at 1.5 ml/min with an ACSF
543 solution. Recordings were obtained using a Multiclamp 700B amplifier (Molecular Devices). Recording

544 electrodes made of borosilicate glass had a resistance of 4-6 MΩ (Warner Instruments, USA) and were
545 filled with K-gluconate solution containing (in mM) 125 K-gluconate, 5 KCl, 10 Hepes, 1 EGTA, 5 Na-
546 phosphocreatine, 0.07 CaCl2, 2 Mg-ATP, 0.4 Na-GTP (pH 7.2, osmolarity 300 mOsm). Only cells with
547 access resistance < 20 MΩ and a change of resistance < 25% over the course of the experiment were
548 analyzed. Data were filtered with a Hum Bug (Quest Scientific, Canada), digitized at 2 kHz (Digidata
549 1444A, Molecular Devices, Sunnyvale, CA, USA), and acquired using Clampex 10 software (Molecular
550 Devices). Whole cell recordings were made from mCherry positive PVT D2 cells visualized with an
551 Olympus microscope (equipped with an mCherry filter). CNO was dissolved in ACSF (10μM, 30 s) and
552 applied in the bath after 10 min baseline recording. The number of action potentials were analyzed
553 before and after CNO application with Clampfit 10 software (Axon Instruments).
554
555 **Statistical Analysis**
556 Data were shown as the mean ± SEM (standard error of the mean). GraphPad Prism v7.0 software was
557 used for statistical analyses. D'Agostino Pearson test is used as a test for normality. When this
558 assumption was not met, non-parametric tests were used (see Table S1). Student's t-test (paired or
559 unpaired, 2-sided) was used to compare two sets of data. Multiple comparisons were performed by 1-
560 way or 2-way ANOVA followed by either Sidak's, Tukey's, Uncorrected Fisher's LSD or Dunn's multiple
561 comparisons were used for *post-hoc* analysis. For comparisons against 0, either one sample t test or
562 Wilcoxon signed rank test (for non-normal data) were used. All statistical comparisons are presented in
563 **Table S1**.
564 In Fig. 4, 1 mCherry animal was excluded for not crossing, 2 hM4Di and 1 mCherry animals were
565 excluded for viral injections outside PVT. In Fig. 5, 1 hM4Di and 1 mCherry animal were excluded for
566 not crossing during the choice-test. In Fig. 6, 1 hM4Di animal was excluded for viral injections outside
567 PVT. In Fig. S6, 2 animals were excluded for spending more than the 75% criterion in one compartment
568 during Pretest.
569
570 **Acknowledgments**
571 We thank all the lab members for comments on the manuscript. We thank M.Verdy and J.Beauduffe for
572 help with behavioral experiments. We warmly thank E.Valjent for sharing the D2-Cre mouse lines. This
573 work was supported by CNRS, INSERM, the IGF, the ATIP-Avenir program (EP), the Bettencourt

Schueller Foundation (EP), the French Research Agency (ANR-19-CE37-0006, ST and LV; ANR-21-CE16-0015, EP, ST, MD and EK), the Human Frontier Science Program Postdoctoral Fellowship (LT0027-2022-L, MM) and Fyssen Foundation (MM). We thank the MRI Biocampus platform and all the Iexplore staff from IGF for their help in the maintenance and breeding of mice.

AUTHOR CONTRIBUTIONS

M.M., E.P. and S.T. conceived the project and designed all the experiments. M.M. performed surgical and anatomical experiments. M.M., L.V., E.K. and M.D. performed behavioral experiments. P.T and J.S. performed and analyzed electrophysiological experiments. The manuscript was written by M.M., E.P. and S.T and commented by all authors.

REFERENCES

1. Rumbaugh, D.M., King, J.E., Beran, M.J., Washburn, D.A., and Gould, K.L. (2007). A Salience Theory of Learning and Behavior: With Perspectives on Neurobiology and Cognition. Int J Primatol *28*, 973–996. https://doi.org/10.1007/s10764-007-9179-8.

2. Domjan, M. (2005). Pavlovian conditioning: a functional perspective. Annu Rev Psychol *56*, 179–206. https://doi.org/10.1146/annurev.psych.55.090902.141409.

3. Rangel, A., Camerer, C., and Montague, P.R. (2008). A framework for studying the neurobiology of value-based decision making. Nat. Rev. Neurosci. *9*, 545–556. https://doi.org/10.1038/nrn2357.

4. Hunter, L.E., and Daw, N.D. (2021). Context-sensitive valuation and learning. Current Opinion in Behavioral Sciences *41*, 122–127. https://doi.org/10.1016/j.cobeha.2021.05.001.

5. Perisse, E., Miranda, M., and Trouche, S. (2023). Modulation of aversive value coding in the vertebrate and invertebrate brain. Current Opinion in Neurobiology *79*, 102696. https://doi.org/10.1016/j.conb.2023.102696.

6. Zweifel, L.S. (2019). Dopamine, uncertainty, and fear generalization. Current Opinion in Behavioral Sciences *26*, 157–164. https://doi.org/10.1016/j.cobeha.2019.01.003.

600 7. Dunsmoor, J.E., and Paz, R. (2015). Fear Generalization and Anxiety: Behavioral and Neural
601 Mechanisms. Biological Psychiatry *78*, 336–343. https://doi.org/10.1016/j.biopsych.2015.04.010.

602 8. Kobayashi, S., and Schultz, W. (2014). Reward Contexts Extend Dopamine Signals to Unrewarded
603 Stimuli. Curr Biol *24*, 56–62. https://doi.org/10.1016/j.cub.2013.10.061.

604 9. Brooks, A.M., Pammi, V.S.C., Noussair, C., Capra, C.M., Engelmann, J.B., and Berns, G.S. (2010).
605 From Bad to Worse: Striatal Coding of the Relative Value of Painful Decisions. Front Neurosci *4*.
606 https://doi.org/10.3389/fnins.2010.00176.

607 10. Villar, M.E., Pavão-Delgado, M., Amigo, M., Jacob, P.F., Merabet, N., Pinot, A., Perry, S.A.,
608 Waddell, S., and Perisse, E. (2022). Differential coding of absolute and relative aversive value in the
609 Drosophila brain. Current Biology *32*, 4576-4592.e5. https://doi.org/10.1016/j.cub.2022.08.058.

610 11. Diederen, K.M.J., Ziauddeen, H., Vestergaard, M.D., Spencer, T., Schultz, W., and Fletcher,
611 P.C. (2017). Dopamine Modulates Adaptive Prediction Error Coding in the Human Midbrain and
612 Striatum. J Neurosci *37*, 1708–1720. https://doi.org/10.1523/JNEUROSCI.1979-16.2016.

613 12. Saez, R.A., Saez, A., Paton, J.J., Lau, B., and Salzman, C.D. (2017). Distinct roles for the
614 amygdala and orbitofrontal cortex in representing the relative amount of expected reward. Neuron
615 *95*, 70-77.e3. https://doi.org/10.1016/j.neuron.2017.06.012.

616 13. Seymour, B., and McClure, S.M. (2008). Anchors, scales and the relative coding of value in the
617 brain. Curr. Opin. Neurobiol. *18*, 173–178. https://doi.org/10.1016/j.conb.2008.07.010.

618 14. Tremblay, L., and Schultz, W. (1999). Relative reward preference in primate orbitofrontal
619 cortex. Nature *398*, 704–708. https://doi.org/10.1038/19525.

620 15. Perisse, E., Yin, Y., Lin, A.C., Lin, S., Huetteroth, W., and Waddell, S. (2013). Different Kenyon
621 Cell Populations Drive Learned Approach and Avoidance in Drosophila. Neuron *79*, 945–956.
622 https://doi.org/10.1016/j.neuron.2013.07.045.

623 16. Rogan, M.T., Leon, K.S., Perez, D.L., and Kandel, E.R. (2005). Distinct Neural Signatures for
624 Safety and Danger in the Amygdala and Striatum of the Mouse. Neuron *46*, 309–320.
625 https://doi.org/10.1016/j.neuron.2005.02.017.

626 17. Kong, M.-S., Ancell, E., Witten, D.M., and Zweifel, L.S. (2024). Valence and Salience Encoding
627 in the Central Amygdala. Preprint, https://doi.org/10.1101/2024.07.05.602310
628 https://doi.org/10.1101/2024.07.05.602310.

629 18. Jacob, P.F., and Waddell, S. (2020). Spaced Training Forms Complementary Long-Term
630 Memories of Opposite Valence in Drosophila. Neuron *106*, 977-991.e4.
631 https://doi.org/10.1016/j.neuron.2020.03.013.

632 19. Nasser, H.M., and McNally, G.P. (2012). Appetitive–aversive interactions in Pavlovian fear
633 conditioning. Behavioral Neuroscience *126*, 404–422. https://doi.org/10.1037/a0028341.

634 20. Felsenberg, J., Jacob, P.F., Walker, T., Barnstedt, O., Edmondson-Stait, A.J., Pleijzier, M.W.,
635 Otto, N., Schlegel, P., Sharifi, N., Perisse, E., et al. (2018). Integration of Parallel Opposing Memories
636 Underlies Memory Extinction. Cell *175*, 709-722.e15. https://doi.org/10.1016/j.cell.2018.08.021.

637 21. Zhang, X., Kim, J., and Tonegawa, S. (2020). Amygdala Reward Neurons Form and Store Fear
638 Extinction Memory. Neuron *105*, 1077-1093.e7. https://doi.org/10.1016/j.neuron.2019.12.025.

639 22. Kirouac, G.J. (2015). Placing the paraventricular nucleus of the thalamus within the brain
640 circuits that control behavior. Neuroscience & Biobehavioral Reviews *56*, 315–329.
641 https://doi.org/10.1016/j.neubiorev.2015.08.005.

642 23. Kirouac, G.J. (2021). The Paraventricular Nucleus of the Thalamus as an Integrating and Relay
643 Node in the Brain Anxiety Network. Front. Behav. Neurosci. *15*.
644 https://doi.org/10.3389/fnbeh.2021.627633.

645 24. Moga, M.M., Weis, R.P., and Moore, R.Y. (1995). Efferent projections of the paraventricular
646 thalamic nucleus in the rat. J Comp Neurol *359*, 221–238. https://doi.org/10.1002/cne.903590204.

647 25. Vertes, R.P., and Hoover, W.B. (2008). Projections of the paraventricular and paratenial nuclei
648 of the dorsal midline thalamus in the rat. Journal of Comparative Neurology *508*, 212–237.
649 https://doi.org/10.1002/cne.21679.

650 26. Li, S., and Kirouac, G.J. (2012). Sources of inputs to the anterior and posterior aspects of the
651 paraventricular nucleus of the thalamus. Brain Struct Funct *217*, 257–273.
652 https://doi.org/10.1007/s00429-011-0360-7.

653 27. Zhu, Y., Nachtrab, G., Keyes, P.C., Allen, W.E., Luo, L., and Chen, X. (2018). Dynamic Salience
654 Processing in Paraventricular Thalamus Gates Associative Learning. Science *362*, 423–429.
655 https://doi.org/10.1126/science.aat0481.

656 28. Garau, C., Liu, X., Calo, G., Schulz, S., and Reinscheid, R.K. (2022). Neuropeptide S Encodes
657 Stimulus Salience in the Paraventricular Thalamus. Neuroscience *496*, 83–95.
658 https://doi.org/10.1016/j.neuroscience.2022.06.013.

659 29. Haight, J.L., Fraser, K.M., Akil, H., and Flagel, S.B. (2015). Lesions of the paraventricular
660 nucleus of the thalamus differentially affect sign- and goal-tracking conditioned responses. European
661 Journal of Neuroscience *42*, 2478–2488. https://doi.org/10.1111/ejn.13031.

662 30. Haight, J.L., Campus, P., Maria-Rios, C.E., Johnson, A.M., Klumpner, M.S., Kuhn, B.N.,
663 Covelo, I.R., Morrow, J.D., and Flagel, S.B. (2020). The lateral hypothalamus and orexinergic
664 transmission in the paraventricular thalamus promote the attribution of incentive salience to reward-
665 associated cues. Psychopharmacology (Berl) *237*, 3741–3758. https://doi.org/10.1007/s00213-020-
666 05651-4.

667 31. Campus, P., Covelo, I.R., Kim, Y., Parsegian, A., Kuhn, B.N., Lopez, S.A., Neumaier, J.F.,
668 Ferguson, S.M., Solberg Woods, L.C., Sarter, M., et al. (2019). The paraventricular thalamus is a
669 critical mediator of top-down control of cue-motivated behavior in rats. eLife *8*, e49041.
670 https://doi.org/10.7554/eLife.49041.

671 32. Gao, C., Leng, Y., Ma, J., Rooke, V., Rodriguez-Gonzalez, S., Ramakrishnan, C., Deisseroth,
672 K., and Penzo, M.A. (2020). Two genetically, anatomically and functionally distinct cell types
673 segregate across anteroposterior axis of paraventricular thalamus. Nat Neurosci *23*, 217–228.
674 https://doi.org/10.1038/s41593-019-0572-3.

675 33. Barson, J.R., Mack, N.R., and Gao, W.-J. (2020). The Paraventricular Nucleus of the Thalamus
676 Is an Important Node in the Emotional Processing Network. Front. Behav. Neurosci. *14*.
677 https://doi.org/10.3389/fnbeh.2020.598469.

678 34. Do-Monte, F.H., Quinones-Laracuente, K., and Quirk, G.J. (2015). A temporal shift in the
679 circuits mediating retrieval of fear memory. Nature *519*, 460–463.
680 https://doi.org/10.1038/nature14030.

681 35. Choi, E.A., Jean-Richard-dit-Bressel, P., Clifford, C.W.G., and McNally, G.P. (2019).
682 Paraventricular Thalamus Controls Behavior during Motivational Conflict. J Neurosci *39*, 4945–4958.
683 https://doi.org/10.1523/JNEUROSCI.2480-18.2019.

684 36. Penzo, M.A., Robert, V., Tucciarone, J., De Bundel, D., Wang, M., Van Aelst, L., Darvas, M.,
685 Parada, L.F., Palmiter, R., He, M., et al. (2015). The paraventricular thalamus controls a central
686 amygdala fear circuit. Nature *519*, 455–459. https://doi.org/10.1038/nature13978.

687 37. Beas, B.S., Wright, B.J., Skirzewski, M., Leng, Y., Hyun, J.H., Koita, O., Ringelberg, N., Kwon,
688 H.-B., Buonanno, A., and Penzo, M.A. (2018). The locus coeruleus drives disinhibition in the midline
689 thalamus via a dopaminergic mechanism. Nat Neurosci *21*, 963–973.
690 https://doi.org/10.1038/s41593-018-0167-4.

691 38. Li, Y., Dong, X., Li, S., and Kirouac, G.J. (2014). Lesions of the posterior paraventricular
692 nucleus of the thalamus attenuate fear expression. Front. Behav. Neurosci. *8*.
693 https://doi.org/10.3389/fnbeh.2014.00094.

694 39. Ma, J., du Hoffmann, J., Kindel, M., Beas, B.S., Chudasama, Y., and Penzo, M.A. (2021).
695 Divergent projections of the paraventricular nucleus of the thalamus mediate the selection of passive
696 and active defensive behaviors. Nat Neurosci *24*, 1429–1440. https://doi.org/10.1038/s41593-021-
697 00912-7.

698 40. Wang, Z., Wang, Z., and Zhou, Q. (2024). Modulation of learning safety signals by acute stress:
699 paraventricular thalamus and prefrontal inhibition. Neuropsychopharmacol. *49*, 961–973.
700 https://doi.org/10.1038/s41386-023-01790-2.

701 41. Salay, L.D., Ishiko, N., and Huberman, A.D. (2018). A midline thalamic circuit determines
702 reactions to visual threat. Nature *557*, 183. https://doi.org/10.1038/s41586-018-0078-2.

703 42. Tolman, E.C. (1939). Prediction of vicarious trial and error by means of the schematic sowbug.
704 Psychological Review *46*, 318–336. https://doi.org/10.1037/h0057054.

705 43. Redish, A.D. (2016). Vicarious trial and error. Nat Rev Neurosci *17*, 147–159.
706 https://doi.org/10.1038/nrn.2015.30.

707 44. Trouche, S., Perestenko, P.V., van de Ven, G.M., Bratley, C.T., McNamara, C.G., Campo-
708 Urriza, N., Black, S.L., Reijmers, L.G., and Dupret, D. (2016). Recoding a cocaine-place memory
709 engram to a neutral engram in the hippocampus. Nat. Neurosci. *19*, 564–567.
710 https://doi.org/10.1038/nn.4250.

711 45. Trouche, S., Koren, V., Doig, N.M., Ellender, T.J., El-Gaby, M., Lopes-Dos-Santos, V., Reeve,
712 H.M., Perestenko, P.V., Garas, F.N., Magill, P.J., et al. (2019). A Hippocampus-Accumbens
713 Tripartite Neuronal Motif Guides Appetitive Memory in Space. Cell *176*, 1393-1406.e16.
714 https://doi.org/10.1016/j.cell.2018.12.037.

715 46. Engelke, D.S., Zhang, X.O., O'Malley, J.J., Fernandez-Leon, J.A., Li, S., Kirouac, G.J.,
716 Beierlein, M., and Do-Monte, F.H. (2021). A hypothalamic-thalamostriatal circuit that controls
717 approach-avoidance conflict in rats. Nat Commun *12*, 2517. https://doi.org/10.1038/s41467-021-
718 22730-y.

719 47. Gao, C., Gohel, C.A., Leng, Y., Ma, J., Goldman, D., Levine, A.J., and Penzo, M.A. (2023).
720 Molecular and spatial profiling of the paraventricular nucleus of the thalamus. eLife *12*, e81818.
721 https://doi.org/10.7554/eLife.81818.

722 48. Rivera-Irizarry, J.K., Hámor, P.U., Rowson, S.A., Asfouri, J., Liu, D., Zallar, L.J., Garcia, A.F.,
723 Skelly, M.J., and Pleil, K.E. (2023). Valence and salience encoding by parallel circuits from the
724 paraventricular thalamus to the nucleus accumbens. Preprint at bioRxiv,
725 https://doi.org/10.1101/2023.07.03.547570 https://doi.org/10.1101/2023.07.03.547570.

49. Do-Monte, F.H., Minier-Toribio, A., Quiñones-Laracuente, K., Medina-Colón, E.M., and Quirk, G.J. (2017). Thalamic Regulation of Sucrose Seeking during Unexpected Reward Omission. Neuron *94*, 388-400.e4. https://doi.org/10.1016/j.neuron.2017.03.036.

50. Choi, E.A., and McNally, G.P. (2017). Paraventricular Thalamus Balances Danger and Reward. J. Neurosci. *37*, 3018–3029. https://doi.org/10.1523/JNEUROSCI.3320-16.2017.

51. Otis, J.M., Zhu, M., Namboodiri, V.M.K., Cook, C.A., Kosyk, O., Matan, A.M., Ying, R., Hashikawa, Y., Hashikawa, K., Trujillo-Pisanty, I., et al. (2019). Paraventricular Thalamus Projection Neurons Integrate Cortical and Hypothalamic Signals for Cue-Reward Processing. Neuron *103*, 423-431.e4. https://doi.org/10.1016/j.neuron.2019.05.018.

52. Robinson, T., and Berridge, K. (2003). Addiction. Annual review of psychology *54*, 25–53. https://doi.org/10.1146/annurev.psych.54.101601.145237.

53. Padoa-Schioppa, C., and Assad, J.A. (2006). Neurons in the orbitofrontal cortex encode economic value. Nature *441*, 223–226. https://doi.org/10.1038/nature04676.

54. Hosokawa, T., Kato, K., Inoue, M., and Mikami, A. (2007). Neurons in the macaque orbitofrontal cortex code relative preference of both rewarding and aversive outcomes. Neurosci. Res. *57*, 434–445. https://doi.org/10.1016/j.neures.2006.12.003.

55. Matsumoto, M., and Hikosaka, O. (2009). How do dopamine neurons represent positive and negative motivational events? Nature *459*, 837–841. https://doi.org/10.1038/nature08028.

56. Steinberg, E.E., Gore, F., Heifets, B.D., Taylor, M.D., Norville, Z.C., Beier, K.T., Földy, C., Lerner, T.N., Luo, L., Deisseroth, K., et al. (2020). Amygdala-Midbrain Connections Modulate Appetitive and Aversive Learning. Neuron *106*, 1026-1043.e9. https://doi.org/10.1016/j.neuron.2020.03.016.

57. Delgado, M.R., Li, J., Schiller, D., and Phelps, E.A. (2008). The role of the striatum in aversive learning and aversive prediction errors. Philos Trans R Soc Lond B Biol Sci *363*, 3787–3800. https://doi.org/10.1098/rstb.2008.0161.

751 58. Menegas, W., Akiti, K., Amo, R., Uchida, N., and Watabe-Uchida, M. (2018). Dopamine
752 neurons projecting to the posterior striatum reinforce avoidance of threatening stimuli. Nat Neurosci
753 *21*, 1421–1430. https://doi.org/10.1038/s41593-018-0222-1.

754 59. Kobayashi, K., Lee, S., Filipowicz, A.L.S., McGaughey, K.D., Kable, J.W., and Nassar, M.R.
755 (2021). Dynamic Representation of the Subjective Value of Information. J Neurosci *41*, 8220–8232.
756 https://doi.org/10.1523/JNEUROSCI.0423-21.2021.

757 60. Knutson, B., Adams, C.M., Fong, G.W., and Hommer, D. (2001). Anticipation of Increasing
758 Monetary Reward Selectively Recruits Nucleus Accumbens. J. Neurosci. *21*, RC159–RC159.
759 https://doi.org/10.1523/JNEUROSCI.21-16-j0002.2001.

760 61. McClure, S.M., Li, J., Tomlin, D., Cypert, K.S., Montague, L.M., and Montague, P.R. (2004).
761 Neural Correlates of Behavioral Preference for Culturally Familiar Drinks. Neuron *44*, 379–387.
762 https://doi.org/10.1016/j.neuron.2004.09.019.

763 62. Preuschoff, K., Bossaerts, P., and Quartz, S.R. (2006). Neural Differentiation of Expected
764 Reward and Risk in Human Subcortical Structures. Neuron *51*, 381–390.
765 https://doi.org/10.1016/j.neuron.2006.06.024.

766 63. Tobler, P.N., O'Doherty, J.P., Dolan, R.J., and Schultz, W. (2007). Reward Value Coding
767 Distinct From Risk Attitude-Related Uncertainty Coding in Human Reward Systems. J Neurophysiol
768 *97*, 1621–1632. https://doi.org/10.1152/jn.00745.2006.

769 64. Constantinople, C.M., Piet, A.T., Bibawi, P., Akrami, A., Kopec, C., and Brody, C.D. (2019).
770 Lateral orbitofrontal cortex promotes trial-by-trial learning of risky, but not spatial, biases. eLife *8*,
771 e49744. https://doi.org/10.7554/eLife.49744.

772 65. John, R.D.S. (1973). Genetic Analysis of Tail Rattling in the Mouse. Nature *241*, 549–551.
773 https://doi.org/10.1038/241549a0.

774 66. Muenzinger, K.F. (1938). Vicarious Trial and Error at a Point of Choice: I. A General Survey of
775 its Relation to Learning Efficiency. The Pedagogical Seminary and Journal of Genetic Psychology
776 *53*, 75–86. https://doi.org/10.1080/08856559.1938.10533799.

67. Hu, D., and Amsel, A. (1995). A simple test of the vicarious trial-and-error hypothesis of hippocampal function. Proc Natl Acad Sci U S A *92*, 5506–5509.

68. Schmidt, B., Hinman, J.R., Jacobson, T.K., Szkudlarek, E., Argraves, M., Escabí, M.A., and Markus, E.J. (2013). Dissociation between Dorsal and Ventral Hippocampal Theta Oscillations during Decision-Making. J. Neurosci. *33*, 6212–6224. https://doi.org/10.1523/JNEUROSCI.2915-12.2013.

69. Steiner, A.P., and Redish, A.D. (2014). Behavioral and neurophysiological correlates of regret in rat decision-making on a neuroeconomic task. Nat Neurosci *17*, 995–1002. https://doi.org/10.1038/nn.3740.

70. Pliota, P., Böhm, V., Grössl, F., Griessner, J., Valenti, O., Kraitsy, K., Kaczanowska, J., Pasieka, M., Lendl, T., Deussing, J.M., et al. (2020). Stress peptides sensitize fear circuitry to promote passive coping. Mol Psychiatry *25*, 428–441. https://doi.org/10.1038/s41380-018-0089-2.

71. Zhu, Y., Wienecke, C.F.R., Nachtrab, G., and Chen, X. (2016). A thalamic input to the nucleus accumbens mediates opiate dependence. Nature *530*, 219–222. https://doi.org/10.1038/nature16954.

72. Zhu, Y.-B., Wang, Y., Hua, X.-X., Xu, L., Liu, M.-Z., Zhang, R., Liu, P.-F., Li, J.-B., Zhang, L., and Mu, D. PBN-PVT projections modulate negative affective states in mice. eLife *11*, e68372. https://doi.org/10.7554/eLife.68372.

73. Hamlin, A.S., Clemens, K.J., Choi, E.A., and McNally, G.P. (2009). Paraventricular thalamus mediates context-induced reinstatement (renewal) of extinguished reward seeking. Eur J Neurosci *29*, 802–812. https://doi.org/10.1111/j.1460-9568.2009.06623.x.

74. Zhang, X., and van den Pol, A.N. (2017). Rapid binge-like eating and body weight gain driven by zona incerta GABA neuron activation. Science *356*, 853–859. https://doi.org/10.1126/science.aam7100.

801 75. Beck, C., and Fibiger, H. (1995). Conditioned fear-induced changes in behavior and in the
802 expression of the immediate early gene c-fos: with and without diazepam pretreatment. J Neurosci
803 *15*, 709–720. https://doi.org/10.1523/JNEUROSCI.15-01-00709.1995.

804 76. Yasoshima, Y., Scott, T.R., and Yamamoto, T. (2007). Differential activation of anterior and
805 midline thalamic nuclei following retrieval of aversively motivated learning tasks. Neuroscience *146*,
806 922–930. https://doi.org/10.1016/j.neuroscience.2007.02.044.

807 77. Igelstrom, K.M., Herbison, A.E., and Hyland, B.I. (2010). Enhanced c-Fos expression in
808 superior colliculus, paraventricular thalamus and septum during learning of cue-reward association.
809 Neuroscience *168*, 706–714. https://doi.org/10.1016/j.neuroscience.2010.04.018.

810 78. Haight, J.L., and Flagel, S.B. (2014). A potential role for the paraventricular nucleus of the
811 thalamus in mediating individual variation in Pavlovian conditioned responses. Front Behav Neurosci
812 *8*. https://doi.org/10.3389/fnbeh.2014.00079.

813 79. Hsu, D.T., Kirouac, G.J., Zubieta, J.-K., and Bhatnagar, S. (2014). Contributions of the
814 paraventricular thalamic nucleus in the regulation of stress, motivation, and mood. Front Behav
815 Neurosci *8*, 73. https://doi.org/10.3389/fnbeh.2014.00073.

816 80. Matzeu, A., Weiss, F., and Martin-Fardon, R. (2015). Transient inactivation of the posterior
817 paraventricular nucleus of the thalamus blocks cocaine-seeking behavior. Neurosci Lett *608*, 34–39.
818 https://doi.org/10.1016/j.neulet.2015.10.016.

819 81. Sangha, S., Robinson, P.D., Greba, Q., Davies, D.A., and Howland, J.G. (2014). Alterations in
820 Reward, Fear and Safety Cue Discrimination after Inactivation of the Rat Prelimbic and Infralimbic
821 Cortices. Neuropsychopharmacology *39*, 2405–2413. https://doi.org/10.1038/npp.2014.89.

822 82. Tao, Y., Cai, C.-Y., Xian, J.-Y., Kou, X.-L., Lin, Y.-H., Qin, C., Wu, H.-Y., Chang, L., Luo, C.-X.,
823 and Zhu, D.-Y. (2020). Projections from Infralimbic Cortex to Paraventricular Thalamus Mediate Fear
824 Extinction Retrieval. Neurosci Bull *37*, 229–241. https://doi.org/10.1007/s12264-020-00603-6.

825 83. Brown, A., and Chaudhri, N. (2023). Optogenetic stimulation of infralimbic cortex projections to
826 the paraventricular thalamus attenuates context-induced renewal. European Journal of
827 Neuroscience *57*, 762–779. https://doi.org/10.1111/ejn.15862.

828 84. Ng, K.H., and Sangha, S. (2022). Encoding of conditioned inhibitors of fear in the infralimbic
829 cortex. Cereb Cortex *33*, 5658–5670. https://doi.org/10.1093/cercor/bhac450.

830 85. Li, S.H., Li, S., and Kirouac, G.J. (2024). Analysis of Monosynaptic Inputs to Thalamic
831 Paraventricular Nucleus Neurons Innervating the Shell of the Nucleus Accumbens and Central
832 Extended Amygdala. Neuroscience *537*, 151–164.
833 https://doi.org/10.1016/j.neuroscience.2023.11.033.

834 86. Meyer, H.C., Odriozola, P., Cohodes, E.M., Mandell, J.D., Li, A., Yang, R., Hall, B.S.,
835 Haberman, J.T., Zacharek, S.J., Liston, C., et al. (2019). Ventral hippocampus interacts with
836 prelimbic cortex during inhibition of threat response via learned safety in both mice and humans.
837 Proceedings of the National Academy of Sciences *116*, 26970–26979.
838 https://doi.org/10.1073/pnas.1910481116.

839 87. Watabe-Uchida, M., Zhu, L., Ogawa, S.K., Vamanrao, A., and Uchida, N. (2012). Whole-Brain
840 Mapping of Direct Inputs to Midbrain Dopamine Neurons. Neuron *74*, 858–873.
841 https://doi.org/10.1016/j.neuron.2012.03.017.

842 88. Glimcher, P.W. (2011). Understanding dopamine and reinforcement learning: The dopamine
843 reward prediction error hypothesis. Proc Natl Acad Sci U S A *108*, 15647–15654.
844 https://doi.org/10.1073/pnas.1014269108.

845 89. Watabe-Uchida, M., and Uchida, N. (2018). Multiple Dopamine Systems: Weal and Woe of
846 Dopamine. Cold Spring Harb. Symp. Quant. Biol. *83*, 83–95.
847 https://doi.org/10.1101/sqb.2018.83.037648.

848 90. Castell, L., Rogliardo, A., Borgne, T.L., Naon, C., Cathala, A., Puighermanal, E., Makrini, L.,
849 Mashhour, N., Petit, C.P., Bernat, C., et al. (2024). Midbrain dopamine D2R regulates the salience
850 of threat-related events. Preprint, https://doi.org/10.1101/2024.11.12.623233
851 https://doi.org/10.1101/2024.11.12.623233.

852 91. Kong, E., Monje, F.J., Hirsch, J., and Pollak, D.D. (2014). Learning not to Fear: Neural
853 Correlates of Learned Safety. Neuropsychopharmacol *39*, 515–527.
854 https://doi.org/10.1038/npp.2013.191.

855 92. Duvarci, S. (2024). Dopaminergic circuits controlling threat and safety learning. Trends in
856 Neurosciences *47*, 1014–1027. https://doi.org/10.1016/j.tins.2024.10.001.

857 93. Li, S., and Kirouac, G.J. (2008). Projections from the paraventricular nucleus of the thalamus
858 to the forebrain, with special emphasis on the extended amygdala. Journal of Comparative
859 Neurology *506*, 263–287. https://doi.org/10.1002/cne.21502.

860 94. Vertes, R.P., Linley, S.B., and Hoover, W.B. (2015). LIMBIC CIRCUITRY OF THE MIDLINE
861 THALAMUS. Neurosci Biobehav Rev *54*, 89–107. https://doi.org/10.1016/j.neubiorev.2015.01.014.

862 95. Van der Werf, Y.D., Witter, M.P., and Groenewegen, H.J. (2002). The intralaminar and midline
863 nuclei of the thalamus. Anatomical and functional evidence for participation in processes of arousal
864 and awareness. Brain Research Reviews *39*, 107–140. https://doi.org/10.1016/S0165-
865 0173(02)00181-9.

866 96. Pinto, A., Jankowski, M., and Sesack, S.R. (2003). Projections from the paraventricular nucleus
867 of the thalamus to the rat prefrontal cortex and nucleus accumbens shell: Ultrastructural
868 characteristics and spatial relationships with dopamine afferents. Journal of Comparative Neurology
869 *459*, 142–155. https://doi.org/10.1002/cne.10596.

870 97. Parsons, M.P., Li, S., and Kirouac, G.J. (2007). Functional and anatomical connection between
871 the paraventricular nucleus of the thalamus and dopamine fibers of the nucleus accumbens. Journal
872 of Comparative Neurology *500*, 1050–1063. https://doi.org/10.1002/cne.21224.

873 98. Kapur, S., Mizrahi, R., and Li, M. (2005). From dopamine to salience to psychosis—linking
874 biology, pharmacology and phenomenology of psychosis. Schizophrenia Research *79*, 59–68.
875 https://doi.org/10.1016/j.schres.2005.01.003.

876 99. De Bundel, D., Zussy, C., Espallergues, J., Gerfen, C.R., Girault, J.-A., and Valjent, E. (2016).
877 Dopamine D2 receptors gate generalization of conditioned threat responses through mTORC1

878 signaling in the extended amygdala. Mol Psychiatry *21*, 1545–1553.
879 https://doi.org/10.1038/mp.2015.210.

880 100. Phelps, E.A., and Sharot, T. (2008). How (and Why) Emotion Enhances the Subjective Sense
881 of Recollection. Curr Dir Psychol Sci *17*, 147–152. https://doi.org/10.1111/j.1467-
882 8721.2008.00565.x.

883 101. Santangelo, V. (2015). Forced to remember: When memory is biased by salient information.
884 Behavioural Brain Research *283*, 1–10. https://doi.org/10.1016/j.bbr.2015.01.013.

885 102. Ghazizadeh, A., and Hikosaka, O. (2022). Salience memories formed by value, novelty and
886 aversiveness jointly shape object responses in the prefrontal cortex and basal ganglia. Nat Commun
887 *13*, 6338. https://doi.org/10.1038/s41467-022-33514-3.

888 103. McGaugh, J.L. (2015). Consolidating Memories. Annual Review of Psychology *66*, 1–24.
889 https://doi.org/10.1146/annurev-psych-010814-014954.

890 104. Sharot, T., Riccardi, A.M., Raio, C.M., and Phelps, E.A. (2007). Neural mechanisms mediating
891 optimism bias. Nature *450*, 102–105. https://doi.org/10.1038/nature06280.

892 105. Colavito, V., Tesoriero, C., Wirtu, A.T., Grassi-Zucconi, G., and Bentivoglio, M. (2015). Limbic
893 thalamus and state-dependent behavior: The paraventricular nucleus of the thalamic midline as a
894 node in circadian timing and sleep/wake-regulatory networks. Neuroscience & Biobehavioral
895 Reviews *54*, 3–17. https://doi.org/10.1016/j.neubiorev.2014.11.021.

896 106. Ren, S., Wang, Y., Yue, F., Cheng, X., Dang, R., Qiao, Q., Sun, X., Li, X., Jiang, Q., Yao, J., et
897 al. (2018). The paraventricular thalamus is a critical thalamic area for wakefulness. Science *362*,
898 429–434. https://doi.org/10.1126/science.aat2512.

899 107. Brewin, C.R. (2001). A cognitive neuroscience account of posttraumatic stress disorder and its
900 treatment. Behaviour Research and Therapy *39*, 373–393. https://doi.org/10.1016/S0005-
901 7967(00)00087-5.

902 108. Layton, B., and Krikorian, R. (2002). Memory mechanisms in posttraumatic stress disorder. J
903 Neuropsychiatry Clin Neurosci *14*, 254–261. https://doi.org/10.1176/jnp.14.3.254.

904 109. Puighermanal Emma, Biever Anne, Espallergues Julie, Gangarossa Giuseppe, De Bundel
905 Dimitri, and Valjent Emmanuel (2014). drd2-cre:ribotag mouse line unravels the possible diversity of
906 dopamine d2 receptor-expressing cells of the dorsal mouse hippocampus. Hippocampus *25*, 858–
907 875. https://doi.org/10.1002/hipo.22408.

908 110. Trouche, S., Sasaki, J.M., Tu, T., and Reijmers, L.G. (2013). Fear extinction causes target-
909 specific remodeling of perisomatic inhibitory synapses. Neuron *80*.
910 https://doi.org/10.1016/j.neuron.2013.07.047.

911 111. Han, S., Soleiman, M.T., Soden, M.E., Zweifel, L.S., and Palmiter, R.D. (2015). Elucidating an
912 Affective Pain Circuit That Creates a Threat Memory. Cell *162*, 363–374.
913 https://doi.org/10.1016/j.cell.2015.05.057.

914

915 **FIGURE LEGENDS**

916

917 **Figure 1. Mice adapt their defensive behavioral responses to safe and aversive conditioning.**
918 (A) Schema of the 1-day conditioned place aversion (CPA) task for the control, safe and aversive
919 groups. Contexts A (square) and B (circle) are connected via a bridge and contain electric shock grids.
920 During conditioning session S1, context A is paired with either 0 mA or four 0.6 mA electric shocks.
921 During conditioning session S2 (30min after S1), context B is paired with either 0 mA or four 0.3 mA
922 electric shocks.
923 (B) Only mice from the aversive group increased their total freezing level during conditioning session
924 S2 compared to S1.
925 (C) Safe and aversive groups, but not the control group, increased freezing before the 1st shock of the
926 conditioning session S2 compared to S1.
927 (D) Freezing after the 4th shock significantly decreased for the safe group between conditioning
928 sessions S1 and S2 while it was maintained for the aversive group.
929 (E) Only the aversive group exhibited tail rattling behavior immediately after the shocks delivered during
930 the conditioning session S2.
931 All data are mean ± SEM. Individual data points are displayed as dots. Control (n=11); safe (n=11);
932 aversive (n=12); *p<0.05; **p<0.01; ***p<0.001; ##p<0.01 against 0, ns: non-significant.

933 See also Figure S1.

934

935 **Figure 2. Mice use prior knowledge and display specific behavioral signatures to make**
936 **appropriate safe and aversive choices.**

937 (A) Percentage of time mice spent in the bridge during the choice-test before and after their 1st cross
938 from context A to context B for the control, safe and aversive groups.

939 (B) Mice from the aversive group spent significantly more time in the bridge before their 1st cross from
940 context $A_{0.6}$ to context $B_{0.3}$ than the control group.

941 (C) Mice from the aversive group made significantly more turnback in the bridge before making their 1st
942 cross from context $A_{0.6}$ to context $B_{0.3}$ than the control and safe groups.

943 (D) After their 1st cross to context B, mice from the safe and aversive groups, but not from the control
944 group, reverted their initial preference (measured during pretest) during the 15 min choice-test, by
945 spending more time in the safest context B as indicated by a positive ΔCPA score (CPA score during
946 the choice test minus CPA score during the pretest).

947 (E) Mice from the aversive group had a specific pattern of freezing during the entire choice-test
948 compared to that of the safe and control groups in the context A (left), bridge (center) and context B
949 (right). The aversive group froze more in the bridge than the safe and control groups. These mice also
950 froze more in context B than the control group.

951 (F) Only mice from the aversive group spent more time in the bridge during the choice test - pretest (Δ
952 Time) after their 1st cross from context A to context B.

953 (G) Mice from both safe and aversive groups spent more time than the control group to cross back from
954 context B to context A during the choice test (i.e. 2nd latency).

955 All data are mean ± SEM. Individual data points are displayed as dots. Control (n=11); safe (n=11);
956 aversive (n=12); *p<0.05; **p<0.01; ***p<0.001. ## p<0.01 and ### p<0.001 against 0; ns: non-
957 significant.

958 See also Figure S2.

959

960 **Figure 3. D2-expressing neurons (D2+) in the anterior PVT are preferentially recruited during**
961 **both safe and aversive conditioning.**

962 (A) Schema of the 1-day conditioned place aversion (CPA) task for the control home cage (HC), safe
963 and aversive groups. Mice were sacrificed 90 min after the conditioning session S2 to assess cFos
964 expression in PVT brain sections.
965 (B) Schematics and representative image of the anterior PVT (aPVT, antero-posterior axis AP: -0.34)
966 showing examples of D2+ (in red) and cFos+ (in white) cells. Scale bar: 100 µm.
967 (C) Both safe and aversive conditioning led to a significant increased cFos density (number of neurons
968 per mm^2) in the aPVT compared to that of the pPVT.
969 (D) D2+ neurons in the aPVT were preferentially recruited after both safe and aversive conditioning
970 compared to home cage control mice.
971 (E-F) The recruitment of D2+ (cFos+D2+ among D2+ cells), but not D2- (cFos+D2- among D2- cells),
972 neurons during aversive conditioning was negatively correlated with the time spent in the bridge during
973 the first 5 minutes of the choice test after the 1st cross. Δ time in the bridge = time in bridge during the
974 choice test minus pretest for the first 5 min after the 1st cross from context A to context B for the aversive
975 (up) and safe (down) groups. Line represents linear regression with confidence interval.
976 All data are mean ± SEM. Individual data points are displayed as dots. Home cage control (n=8); safe
977 (n=10); aversive (n=10); *p<0.05; **p<0.01.
978 See also Figure S3.
979
980 **Figure 4. D2-expressing neurons are required for aversive evaluation and choice.**
981 (A) D2-Cre mice were injected in the aPVT with either DIO-mCherry or DIO-hM4Di-mCherry viral vector
982 (left panel). Representative image of mCherry expression in the aPVT (right panel). Scale bar: 100 µm.
983 (B) Schema of the 1-day condition place aversion (CPA) task for the aversive group. Control mCherry
984 and hM4Di mice were i.p. injected with CNO (2mg/kg) 30 min before the conditioning session S2 in
985 Context $B_{0.3}$ and were tested 1h later during a choice-test.
986 (C) hM4Di mice exhibited higher tail rattling after each shock of the conditioning session S2.
987 (D) While the distance travelled immediately after shock decreased during the conditioning S2
988 compared to S1 for mCherry control mice, hM4Di mice did not show such reduced distance during S2.
989 (E) hM4Di mice showed increased turnback in the bridge before their 1st cross from context $A_{0.6}$ to
990 context $B_{0.3}$.

991 (F) hM4Di mice exhibited increased tail rattling behavior before their 1st cross from context $A_{0.6}$ to
992 context $B_{0.3}$.
993 (G) ΔCPA score (CPA score during the choice test - CPA score during the pretest) was significantly
994 decreased for hM4Di mice during the 15 min choice test, with mice preferring none of the 2 contexts.
995 (H) hM4Di mice spent significantly more time in the bridge after their 1st cross from context $A_{0.6}$ to
996 context $B_{0.3}$.
997 (I) hM4Di mice significantly decreased their freezing during the 15 min choice test in context $B_{0.3}$. All
998 tests are comparisons between mCherry control and hM4Di for each compartment.
999 (J) hM4Di mice significantly decreased their 2nd latency to cross back from context $B_{0.3}$ to context $A_{0.6}$
1000 during the choice test.
1001 All data are mean ± SEM. Individual data points are displayed as dots. mCherry control (n=8); hM4Di
1002 (n=8); *p<0.05; **p<0.01; ***p<0.001; ###: p<0.001 difference from 0; ns: non-significant.
1003 See also Figure S4.
1004
1005 **Figure 5. Inhibiting aPVT D2 neurons increases contextual aversiveness and related threat-**
1006 **predicting behavioral traits.**
1007 (A) Schema of the 1-day condition place aversion task in which both A and B contexts are paired with
1008 0.3mA. Control mCherry and hM4Di mice were i.p. injected with CNO (2mg/kg) 30 min before the
1009 conditioning session S2.
1010 (B) hM4Di mice displayed a greater number of tail rattling during conditioning session 2 compared to
1011 mCherry control mice.
1012 (C) Freezing changes between S1 and S2 after the 4th shock tend to be similar between hM4Di and
1013 mCherry mice.
1014 (D) hM4Di displayed more turnback in the bridge before the 1st cross from context $A_{0.3}$ to context $B_{0.3}$
1015 than mCherry control mice.
1016 (E) hM4Di and mCherry control mice showed a similar 1st latency to cross from context $A_{0.3}$ to context
1017 $B_{0.3}$.
1018 (F) hM4Di mice and mCherry control mice spent a similar amount of time in the bridge before their 1st
1019 cross between context $A_{0.3}$ to context $B_{0.3}$.

1020 (G) hM4Di and mCherry control mice froze similarly in the context $A_{0.3}$, bridge and $B_{0.3}$ during the choice
1021 test. All tests are comparisons between mCherry control and hM4Di for each compartment.
1022 (H) ΔCPA score (CPA score during the choice test - CPA score during the pretest) during the 15 min
1023 choice test is significantly lower and not different from 0 in hM4Di mice compared to that of mCherry
1024 control mice.
1025 All data are mean ± SEM. Individual data points are displayed as dots. mCherry control (n=8); hM4Di
1026 (n=7); (*) p=0.0565; *P<0.05; ***p<0.001; #P<0.05; ns: non-significant.
1027 See also Figure S5.
1028
1029 **Figure 6. Inhibiting aPVT D2 neurons increases contextual safeness and related safety-**
1030 **predicting behavioral traits.**
1031 (A) Schema of the 1-day condition place aversion task for the safe group. Control mCherry and hM4Di
1032 mice were i.p. injected with CNO (2mg/kg) 30 min before the conditioning session S2.
1033 (B) hM4Di mice did not change the number of tail rattling during conditioning.
1034 (C) hM4Di and control mCherry mice similarly showed a decreased distance after shock between S1
1035 and S2.
1036 (D) hM4Di and control mCherry mice showed a similar number of turnback in the bridge before 1st cross
1037 from context $A_{0.6}$ to context B_0.
1038 (E) hM4Di and control mCherry mice exhibited a similar number of tail rattling before 1st cross from
1039 context $A_{0.6}$ to context B_0.
1040 (F) hM4Di mice did not change the 1st latency to cross from context $A_{0.6}$ to context B_0.
1041 (G) hM4Di mice significantly increased their 2nd latency to cross back from the context B_0 to the context
1042 $A_{0.6}$ during the choice test.
1043 (H) During the choice test, hM4Di mice significantly decreased freezing in context $A_{0.6}$, increased their
1044 freezing in context B_0, with no change in freezing in the bridge. All tests are comparisons between
1045 mCherry control and hM4Di for each compartment.
1046 (I) hM4Di mice significantly increased their ΔCPA score (CPA score during the choice test - CPA score
1047 during the pretest) during the 15 min choice test.
1048 All data are mean ± SEM. Individual data points are displayed as dots. mCherry control (n=8); hM4Di
1049 (n=8); ##P<0.01 against 0; ### p<0.001 against 0; *p<0.05; **p<0.01; ns: non-significant.

1050 See also Figure S6.

1051

1052

Figure 1

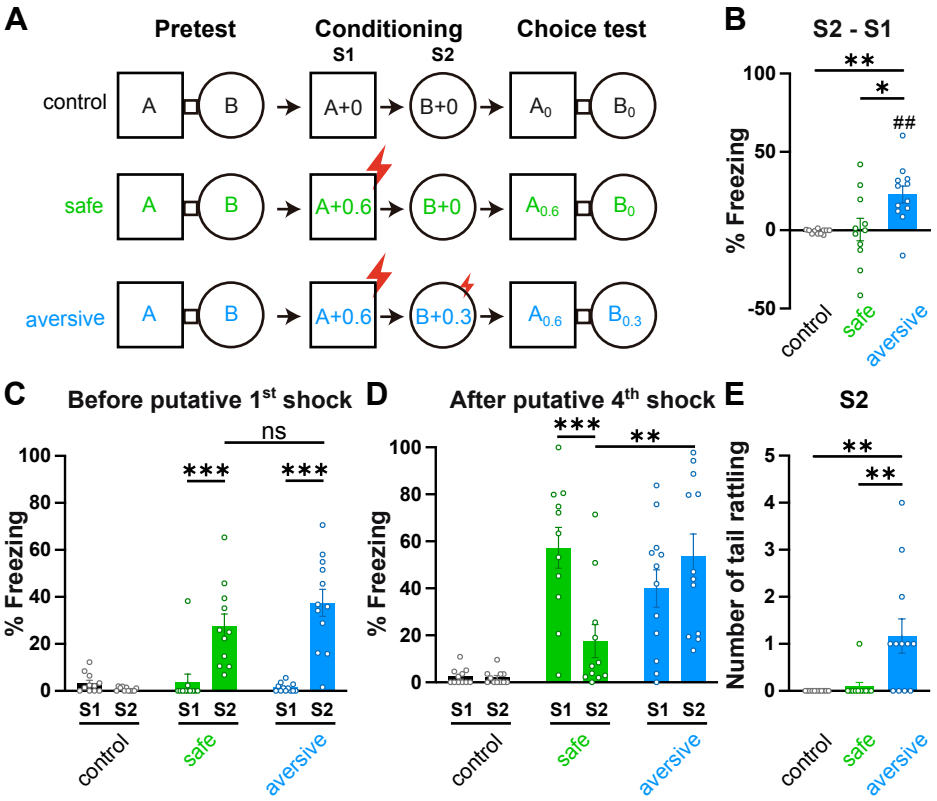
A
Pretest
Conditioning
S1
S2
Choice test
control
safe
aversive
A
B
A+0
B+0
A0
B0
A+0.6
B+0
A0.6
B0
A+0.6
B+0.3
A0.6
B0.3
B
S2 - S1
% Freezing
100
50
0
-50
**
*
##
control
safe
aversive
C
Before putative 1st shock
% Freezing
100
80
60
40
20
0
ns
***
***
S1 S2
S1 S2
S1 S2
control
safe
aversive
D
After putative 4th shock
% Freezing
100
80
60
40
20
0
***
**
S1 S2
S1 S2
S1 S2
control
safe
aversive
E
S2
Number of tail rattling
5
4
3
2
1
0
**
**
control
safe
aversive

Figure 2

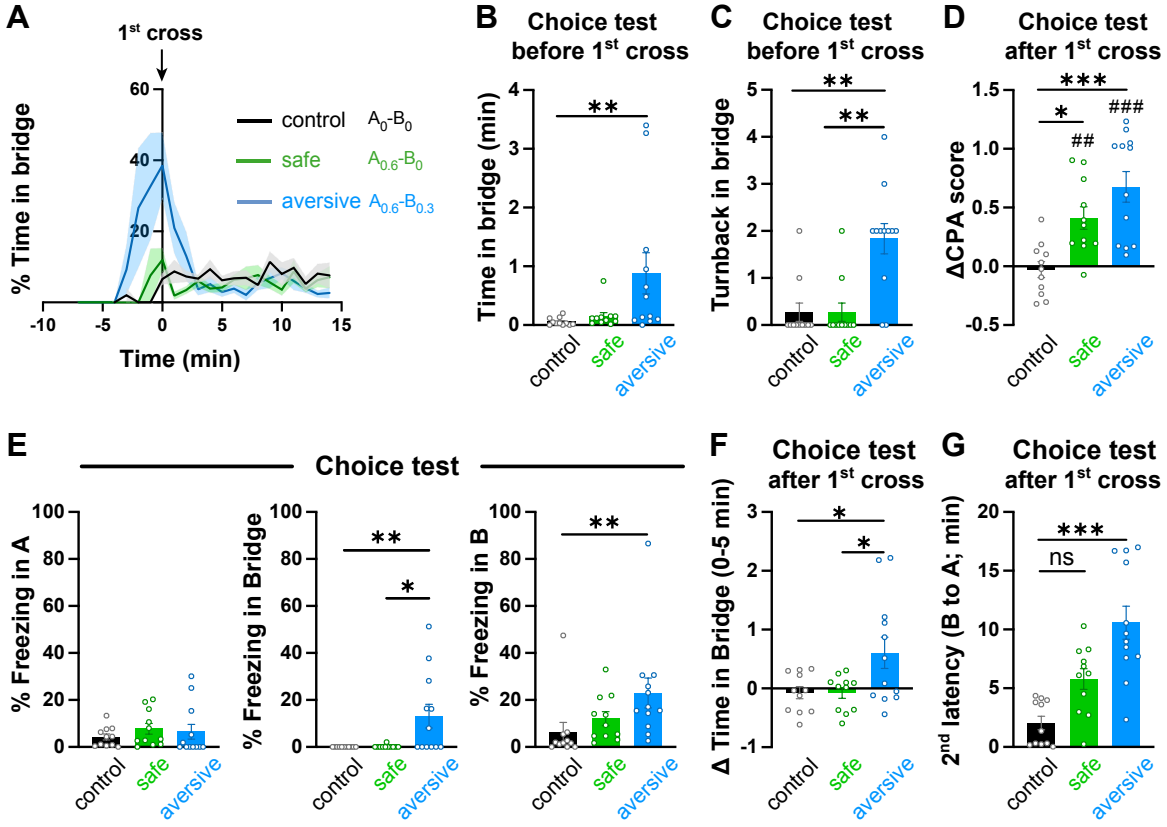
A
1st cross
% Time in bridge
Time (min)
control A0-B0
safe A0.6-B0
aversive A0.6-B0.3
B
Choice test before 1st cross
Time in bridge (min)
C
Choice test before 1st cross
Turnback in bridge
D
Choice test after 1st cross
ΔCPA score
E
Choice test
% Freezing in A
% Freezing in Bridge
% Freezing in B
F
Choice test after 1st cross
Δ Time in Bridge (0-5 min)
G
Choice test after 1st cross
2nd latency (B to A; min)
control
safe
aversive
ns

Figure 3

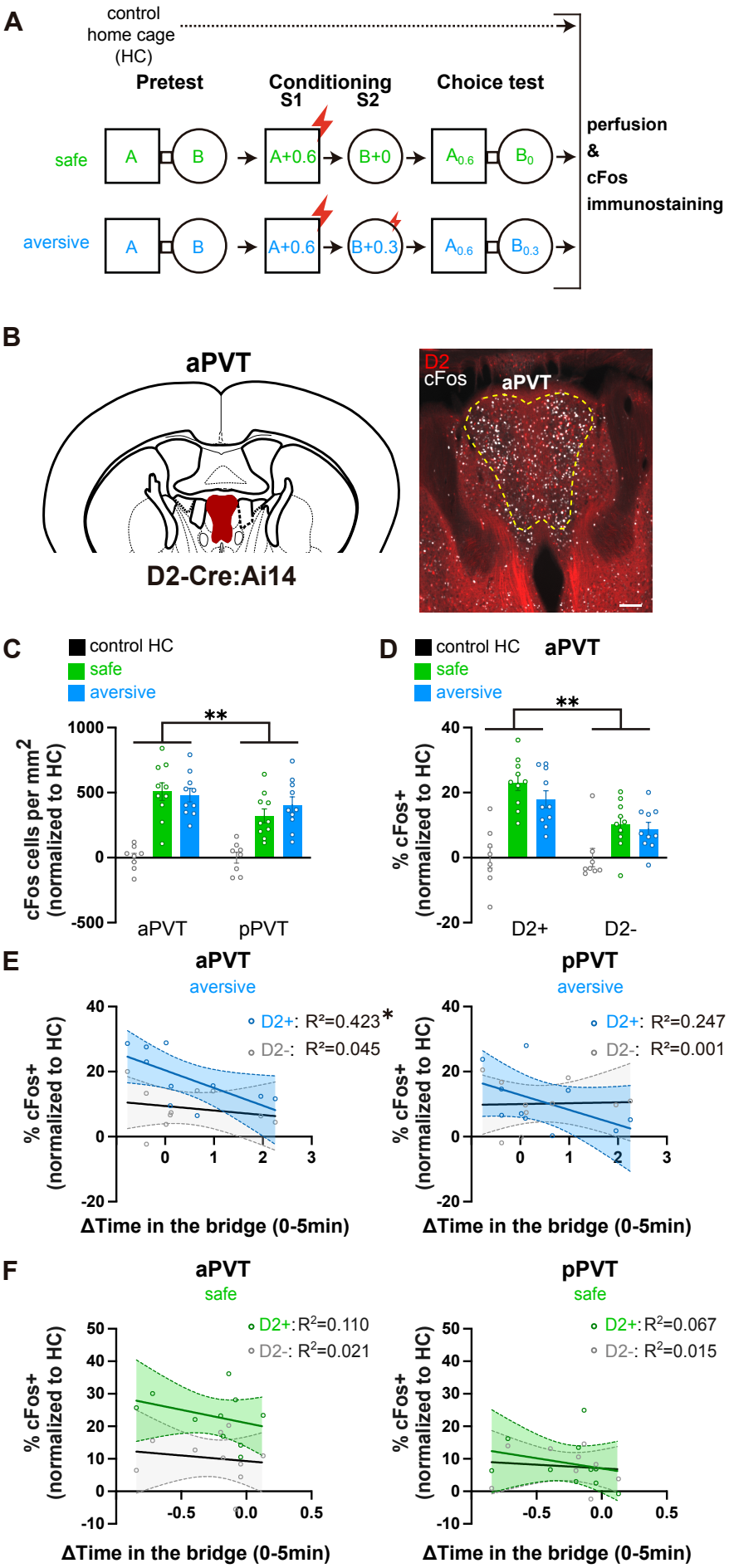
A
control
home cage
(HC)
Pretest
Conditioning
S1
S2
Choice test
safe
A
B
A+0.6
B+0
A0.6
B0
aversive
A
B
A+0.6
B+0.3
A0.6
B0.3
perfusion
&
cFos
immunostaining
B
aPVT
D2-Cre:Ai14
D2
cFos
aPVT
C
control HC
safe
aversive
**
cFos cells per mm2
(normalized to HC)
1000
500
0
-500
aPVT
pPVT
D
control HC
aPVT
safe
aversive
**
% cFos+
(normalized to HC)
40
20
0
-20
D2+
D2-
E
aPVT
aversive
D2+: R²=0.423*
D2-: R²=0.045
% cFos+
(normalized to HC)
ΔTime in the bridge (0-5min)
pPVT
aversive
D2+: R²=0.247
D2-: R²=0.001
% cFos+
(normalized to HC)
ΔTime in the bridge (0-5min)
F
aPVT
safe
D2+: R²=0.110
D2-: R²=0.021
% cFos+
(normalized to HC)
ΔTime in the bridge (0-5min)
pPVT
safe
D2+: R²=0.067
D2-: R²=0.015
% cFos+
(normalized to HC)
ΔTime in the bridge (0-5min)

Figure 4

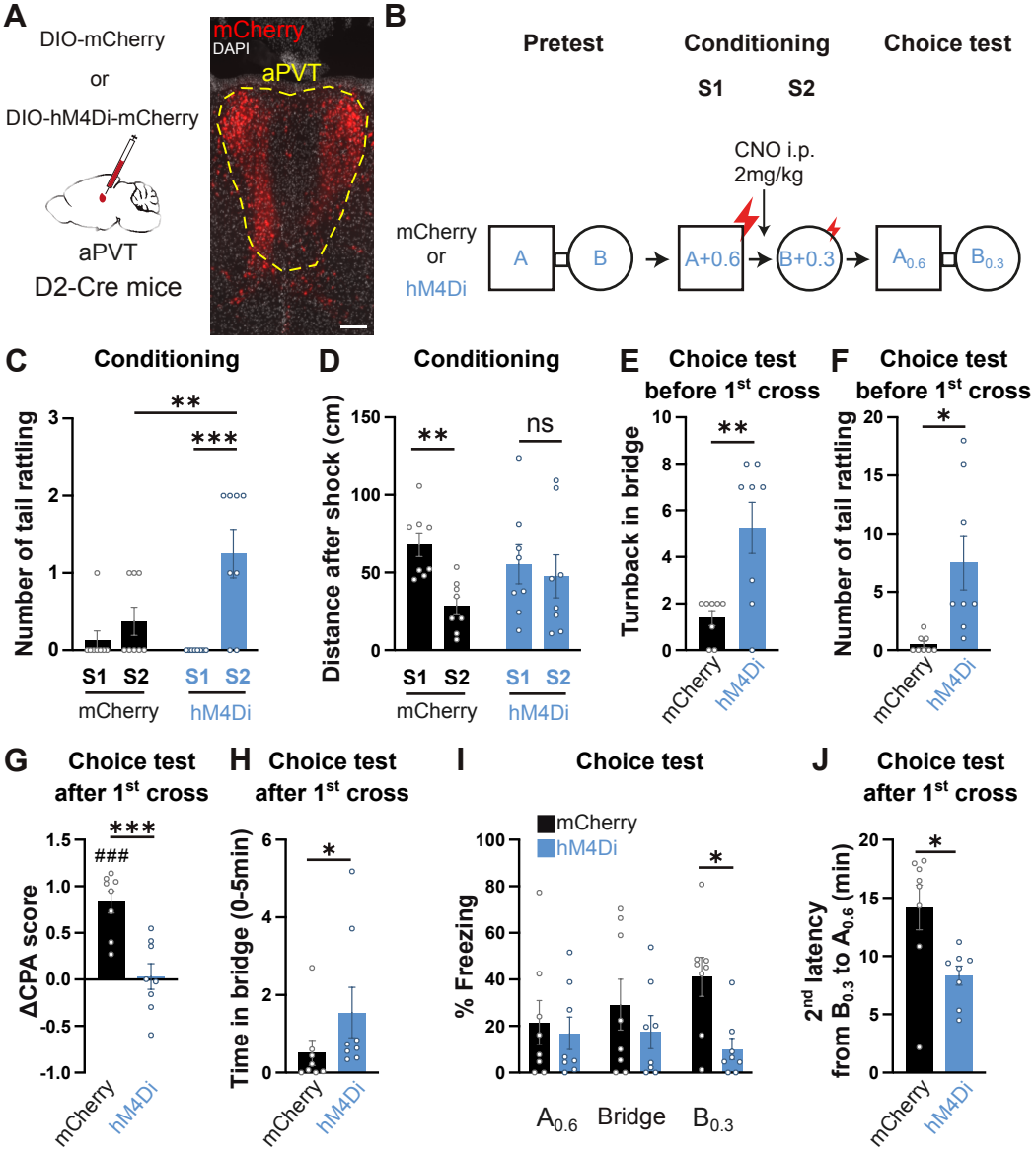
A
DIO-mCherry
or
DIO-hM4Di-mCherry
aPVT
D2-Cre mice
mCherry
DAPI
aPVT
B
Pretest
Conditioning
Choice test
S1
S2
CNO i.p.
2mg/kg
mCherry
or
hM4Di
A
B
A+0.6
B+0.3
A0.6
B0.3
C
Conditioning
Number of tail rattling
S1 S2 S1 S2
mCherry hM4Di
D
Conditioning
Distance after shock (cm)
ns
E
Choice test
before 1st cross
Turnback in bridge
F
Choice test
before 1st cross
Number of tail rattling
G
Choice test
after 1st cross
ΔCPA score
###
H
Choice test
after 1st cross
Time in bridge (0-5min)
I
Choice test
mCherry
hM4Di
% Freezing
A0.6
Bridge
B0.3
J
Choice test
after 1st cross
2nd latency
from B0.3 to A0.6 (min)

Figure 5

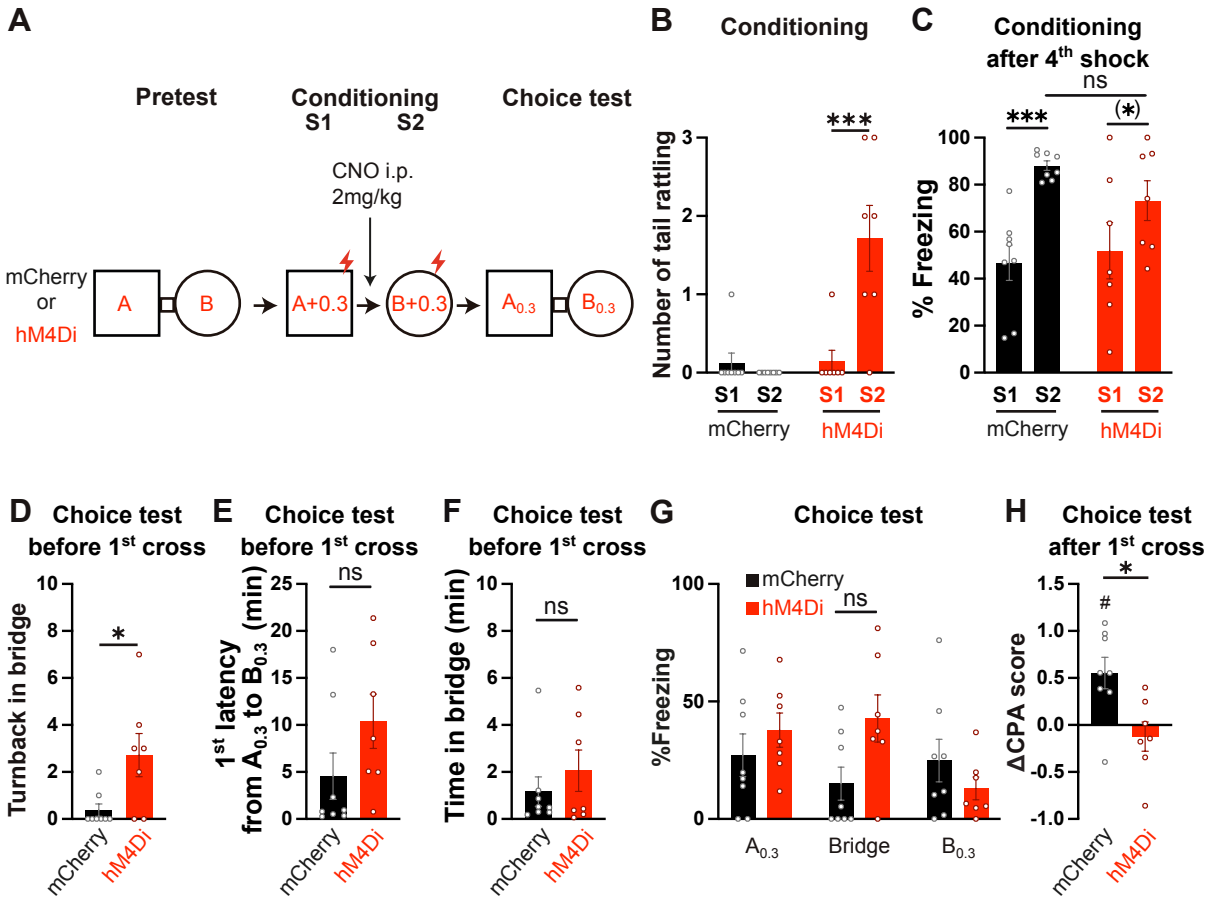
A
Pretest
Conditioning
S1
S2
Choice test
CNO i.p.
2mg/kg
mCherry
or
hM4Di
A
B
A+0.3
B+0.3
A0.3
B0.3
B
Conditioning
Number of tail rattling
***
S1
S2
S1
S2
mCherry
hM4Di
C
Conditioning
after 4th shock
ns
***
(*)
% Freezing
S1
S2
S1
S2
mCherry
hM4Di
D
Choice test
before 1st cross
Turnback in bridge
*
mCherry
hM4Di
E
Choice test
before 1st cross
ns
1st latency
from A0.3 to B0.3 (min)
mCherry
hM4Di
F
Choice test
before 1st cross
ns
Time in bridge (min)
mCherry
hM4Di
G
Choice test
mCherry
hM4Di
ns
%Freezing
A0.3
Bridge
B0.3
H
Choice test
after 1st cross
*
#
ΔCPA score
mCherry
hM4Di

Figure 6

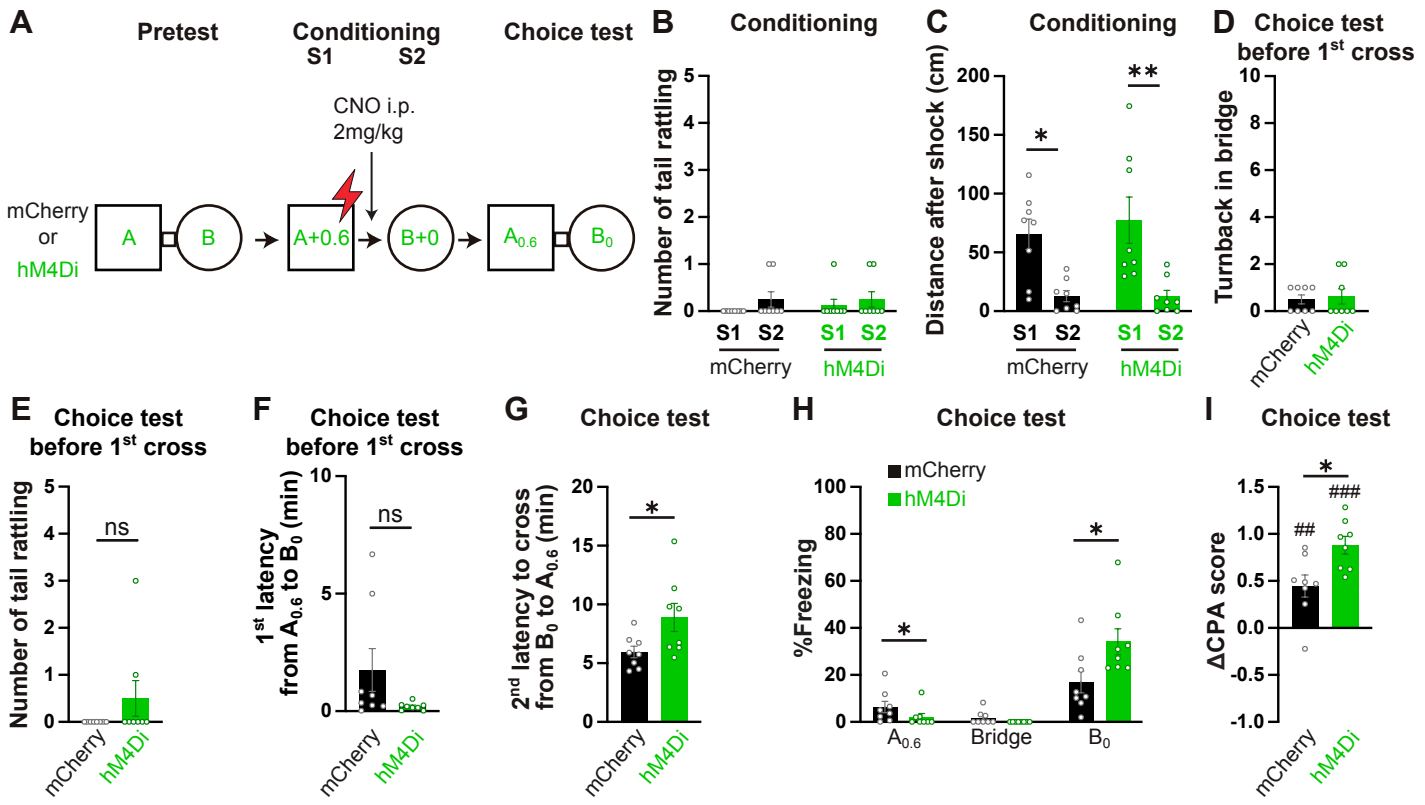
A
Pretest
Conditioning
S1 S2
Choice test
CNO i.p.
2mg/kg
mCherry
or
hM4Di
A
B
A+0.6
B+0
A0.6
B0
B
Conditioning
Number of tail rattling
S1 S2 S1 S2
mCherry hM4Di
C
Conditioning
Distance after shock (cm)
*
**
S1 S2 S1 S2
mCherry hM4Di
D
Choice test
before 1st cross
Turnback in bridge
mCherry hM4Di
E
Choice test
before 1st cross
Number of tail rattling
ns
mCherry hM4Di
F
Choice test
before 1st cross
1st latency
from A0.6 to B0 (min)
ns
mCherry hM4Di
G
Choice test
2nd latency to cross
from B0 to A0.6 (min)
*
mCherry hM4Di
H
Choice test
mCherry
hM4Di
%Freezing
*
*
A0.6 Bridge B0
I
Choice test
ΔCPA score
*
##
###
mCherry hM4Di